



Review

# The Incremental Role of Multiorgan Point-of-Care Ultrasounds in the Emergency Setting

Antonello D'Andrea <sup>1,\*</sup>, Carmen Del Giudice <sup>2</sup> , Dario Fabiani <sup>2</sup> , Adriano Caputo <sup>2</sup>, Francesco Sabatella <sup>2</sup>, Luigi Cante <sup>2</sup>, Stefano Palermi <sup>3</sup>, Alfonso Desiderio <sup>1</sup>, Ercole Tagliamonte <sup>1</sup>, Biagio Liccardo <sup>2</sup> and Vincenzo Russo <sup>2</sup>

<sup>1</sup> Department of Cardiology and Intensive Coronary Care, Umberto I Hospital, 84014 Nocera Inferiore, Italy  
<sup>2</sup> Division of Cardiology, Department of Translational Medical Sciences, University of Campania Luigi Vanvitelli, 80131 Naples, Italy  
<sup>3</sup> Public Health Department, University of Naples Federico II, 80131 Naples, Italy  
\* Correspondence: antonellodandrea@libero.it

**Abstract:** Point-of-care ultrasonography (POCUS) represents a goal-directed ultrasound examination performed by clinicians directly involved in patient healthcare. POCUS has been widely used in emergency departments, where US exams allow physicians to make quick diagnoses and to recognize early life-threatening conditions which require prompt interventions. Although initially meant for the real-time evaluation of cardiovascular and respiratory pathologies, its use has been extended to a wide range of clinical applications, such as screening for deep-vein thrombosis and trauma, abdominal ultrasonography of the right upper quadrant and appendix, and guidance for invasive procedures. Moreover, recently, bedside ultrasounds have been used to evaluate the fluid balance and to guide decongestive therapy in acutely decompensated heart failure. The aim of the present review was to discuss the most common applications of POCUS in the emergency setting.

**Keywords:** POCUS; point-of-care; emergency medicine (EM); echocardiography; lung ultrasound (LUS); VE x US; congestion; deep-vein thrombosis (DTV)



**Citation:** D'Andrea, A.; Del Giudice, C.; Fabiani, D.; Caputo, A.; Sabatella, F.; Cante, L.; Palermi, S.; Desiderio, A.; Tagliamonte, E.; Liccardo, B.; et al. The Incremental Role of Multiorgan Point-of-Care Ultrasounds in the Emergency Setting. *Int. J. Environ. Res. Public Health* **2023**, *20*, 2088. <https://doi.org/10.3390/ijerph20032088>

Academic Editor: Paul B. Tchounwou

Received: 30 November 2022

Revised: 10 January 2023

Accepted: 13 January 2023

Published: 23 January 2023



**Copyright:** © 2023 by the authors. Licensee MDPI, Basel, Switzerland. This article is an open access article distributed under the terms and conditions of the Creative Commons Attribution (CC BY) license (<https://creativecommons.org/licenses/by/4.0/>).

## 1. Introduction

In 2001, the American College of Emergency Physicians (ACEP) published the first Emergency Ultrasound Guidelines with the aim to describe the principal point-of-care ultrasonography (POCUS) applications and to underline the importance of continuing education and training in the use of emergency ultrasounds. These guidelines then expanded together with the growing use of focused ultrasounds [1]. POCUS represents an important diagnostic tool which is performed at the bedside, thus allowing physicians to rapidly evaluate patients admitted into the emergency department (ED) and to make clinical decisions [2]. POCUS is used for goal-directed echocardiography, lung ultrasounds, screening for deep-vein thrombosis in people suspected to have a pulmonary embolism, abdominal ultrasonography, intracranial pressure and trauma monitoring, and guidance for invasive procedures [3,4]. The aim of this review was to summarize the most common applications of POCUS in the emergency setting.

## 2. Lung Ultrasounds in the Emergency Department

### 2.1. Technical Equipment and Methodology

Lung ultrasound (LUS) examinations can be performed with the use of probes of different frequencies based on the lung region to be explored. A high-frequency (7.5–10 MHz) linear probe, thanks to it having a greater spatial resolution than its depth of penetration, is useful for performing a detailed exam of the chest wall and pleurae. Conversely, a low-frequency (3.5–5 MHz) curvilinear probe has a greater depth of penetration and is

suitable for examining the parenchymal structures below the pleurae. Lichtenstein et al. [5] recommended the use of a 5 MHz microconvex probe for bedside LUSs. Many studies suggest the use of a single probe for a complete LUS examination in the emergency and critical care setting [6]. The probes are placed over the intercostal spaces along the longitudinal plane, perpendicular to the ribs [7,8], offering an acoustic window into the lung parenchyma. The 2012 and 2022 international consensuses have proposed an eight-region model for LUS examinations in the emergency department [6,8]. Based on this protocol, each hemithorax is divided into two anterior and lateral regions by the parasternal line and the anterior and posterior axillary lines. Each of these regions is subdivided into upper and basal segments, leading to a total of eight regions. Alternatively, Lichtenstein et al. proposed the Bedside Lung Ultrasound in Emergency (BLUE) protocol for LUS examinations of patients presenting to the emergency department with dyspnea [5]. The BLUE protocol identifies three points of interest per hemithorax to be examined, or so-called BLUE points [5], and quickly provides three clinical diagnostic profiles. LUS examinations include two main modalities: B-mode (brightness mode), which generates two-dimensional images, and M-mode, which is useful for examining the motion of the lung surfaces towards and away from the probe. Doppler techniques are not usually used in a standard exam. Moreover, LUS examinations are based on two types of images: artifacts and real images. Artifacts (A-lines and B-lines) could be normal or pathological. They are due to the higher acoustic impedance differences between the air and the superficial lung tissues and are generated by the pleural surface [9]. Conversely, real images (such as pleural effusion and lung consolidations) are always pathological signs.

## 2.2. Pleural Disorders

### 2.2.1. Pneumothorax

LUS examinations allow for the detection of trapped air within the pleural space. Three signs are suggestive of a pneumothorax (PNX) diagnosis.

#### (A) Abolition of lung sliding

Lung sliding is represented by the physiological movement of the parietal pleura against the visceral pleura during the respiratory cycle, which is visualized in B-mode images [10]. The abolition of lung sliding suggests a PNX with a high negative predictive value (sensitivity of 95% and negative predictive value of 100%) in the general population [11], while its presence can accurately rule out a PNX diagnosis (sensitivity of 95%, specificity of 91%, and negative predictive value of 100%) [11]. Atelectasis, one-lung intubation, acute respiratory distress syndrome (ARDS), pneumonia, pulmonary fibrosis, and cardiopulmonary arrest, which reduce regional lung ventilation, can cause false-positive diagnoses. For this reason, the positive predictive value of lung sliding abolition for PNX diagnoses is reduced to 56% in critically ill patients [12] and to 27% in the case of acute respiratory failure [5]. Hence, the abolition of lung sliding is not always suggestive of a PNX, and this sign, when isolated, is not sufficient for PNX diagnoses.

#### (B) A-lines

A-lines are horizontal hyperechoic lines localized below the pleural line and repeated at equal intervals (Figure 1). They represent the reverberation artifacts arising from the pleurae and correspond to normal lung ventilation [13]. A-lines are always present in PNXs (sensitivity of 100%) [14] but are not specific because they are also generated by physiological aeration or other pathological conditions (such as chronic obstructive pulmonary disease (COPD) exacerbation and obstructed airways). An A-line presence with the associated abolition of lung sliding is highly suggestive of a PNX in trauma patients (sensitivity of 98% and specificity of 99%) [15].



**Figure 1.** A-lines (arrow).

### (C) Lung point

In the M-mode view, the “seashore sign” is defined as the presence of straight lines above the pleural line with an associated granular pattern below it. This sign confirms lung ventilation and sliding [5] and could be helpful in the critical care setting, where sliding is reduced or absent [16]. Conversely, the absence of pleural movement during respiratory cycles causes straight lines both above and below the pleural line, a pattern defined as the “stratosphere sign”, in the M-mode view. The lung point is defined as the point where the normal lung (“seashore sign”) replaces the PNX air trapped (“stratosphere sign”) during deep inspiration (Figure 2) [17]. Its position must be searched for with a probe in the thorax. This sign is specific for PNX diagnoses (sensitivity of 66% and specificity of 100%) [12] and allows a semiquantitative evaluation of PNX extension (>30% if localized below the midaxillary line) [13].

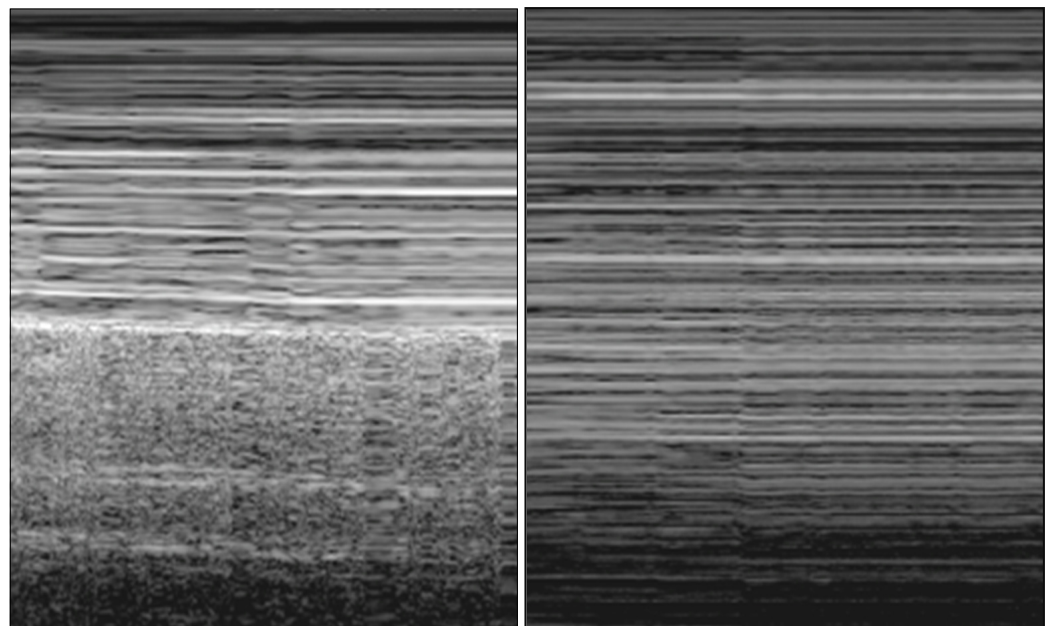


**Figure 2.** Lung point: “seashore sign” (left) turns into “stratosphere sign” (right) in M-mode view during deep inspiration.

### 2.2.2. Pleural Effusion

Pleural effusion is defined as a hypoechoic/anechoic structure without the presence of air inside which presents during expiration and inspiration (Figure 3) [18]. The probe is placed on the posterior region behind the posterior axillary line of a supine patient. In the critical care setting, when it is not always possible to distinguish the pathognomonic hypoechoic/anechoic structure (such as in case of a hemothorax or pyothorax), it could be useful to look for the “sinusoid sign”, which consists in the movement of the lung towards the pleural line during inspiration and away from the pleural line during expiration [19]. LUSs allow for the detection of pleural effusion with a high diagnostic accuracy (sensitivity of 93% and specificity of 97%) [20]; in addition, the “sinusoid sign” presents a high specificity for pleural effusion diagnoses (specificity of 97%) [21]. Various studies have supported that LUSs have a better diagnostic accuracy than chest X-rays (CXR) for evaluating pleural effusion [6,22]. When pleural effusion is abundant, the adjacent lung region is seen to be consolidated and floating within the pleural space [23]. In the presence of pleural effusion localized in the basal lung regions, it is possible to identify, as anatomical landmarks, the spleen, liver, and diaphragm. A color Doppler showing the intrasplenic and intrahepatic blood vessels is a useful tool for distinguishing the spleen and liver tissues from pleural effusion. LUS examinations also allow for the quantification of pleural effusion: a distance between the lung and posterior chest wall, measured at the lung basal regions during end-expiration or end-inspiration with the patient in a supine position, of  $\geq 50$  mm is highly predictive of a pleural effusion volume of  $\geq 500$  mL [24,25]. There is a high correlation degree between the pleural effusion volume assessed through computed tomography (CT) and that which was assessed through an LUS exam [26]. Finally, LUS exams allow for guidance during thoracentesis procedures at the bedside with a high success rate [27].

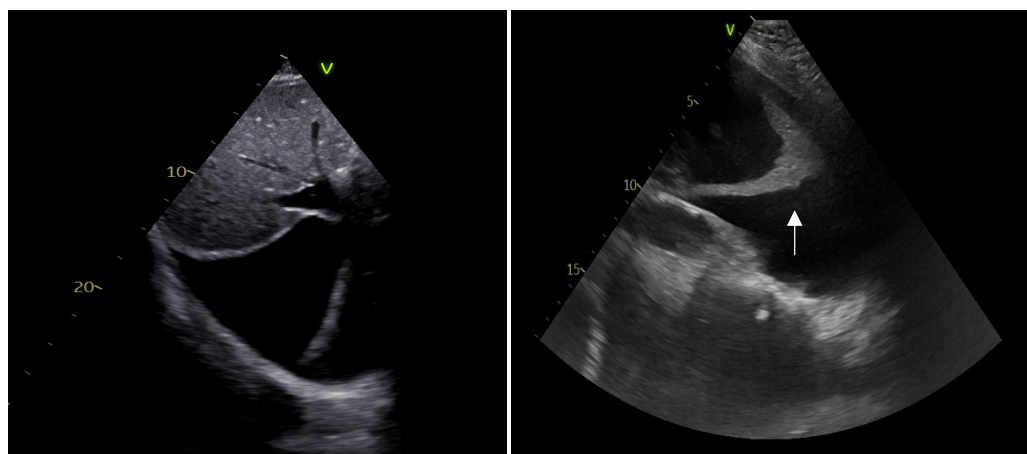


**Figure 3.** Pleural effusion with lung region floating inside (arrow).

### 2.3. Lung Parenchymal Disorders

#### 2.3.1. Interstitial Syndrome

B-lines are vertical hyperechoic lines derived from the pleural line (Figure 4), obliterating physiological A-lines and moving synchronously with lung sliding until the edge of the screen [6,19]. They are artifacts that appear due to the interaction of the ultrasound with the air–fluid interface of the lung tissue, and their presence correlates with thickened subpleural interlobular septa [14]. A maximum of two B-lines per scan can be present in physiological conditions [9]. The presence of B-lines allows one to rule out a PNX diagnosis with a high negative predictive value (sensitivity of 100%, specificity of 60%, and negative predictive value of 100%) [14]. An increased number of B-lines is associated with an impaired air–tissue ratio of the examined lung area and with a strong correlation with the tissue density measured through CT [13]. The presence of three or more B-lines per scan without A-lines is always pathological and indicates a specific pattern called a “B-pattern” [28]. This

ultrasonographic pattern is suggestive of an interstitial syndrome diagnosis (93% accuracy compared with CXR and 100% compared with CT) [9], also allowing differential diagnoses of COPD exacerbation (sensitivity of 100% and specificity of 92%) [25,29]. The number of B-lines per scan correlates with the degree of lung aeration loss [9,20]. The distribution of lung B-lines allows for the evaluation of the differential diagnoses of various clinical conditions [8,30]. The presence of a diffuse B-pattern (at least two regions per hemithorax) with a homogeneous and gravitational (basal-to-apex gradient) distribution, regular thin pleurae, and normal sliding indicates cardiogenic edema [31]. Conversely, a diffuse B-pattern with a nonhomogeneous distribution (surfaces of normal lung parenchyma spared), irregular and thickened pleurae, anterior subpleural consolidations, and absent or reduced lung sliding points to ARDS [31].

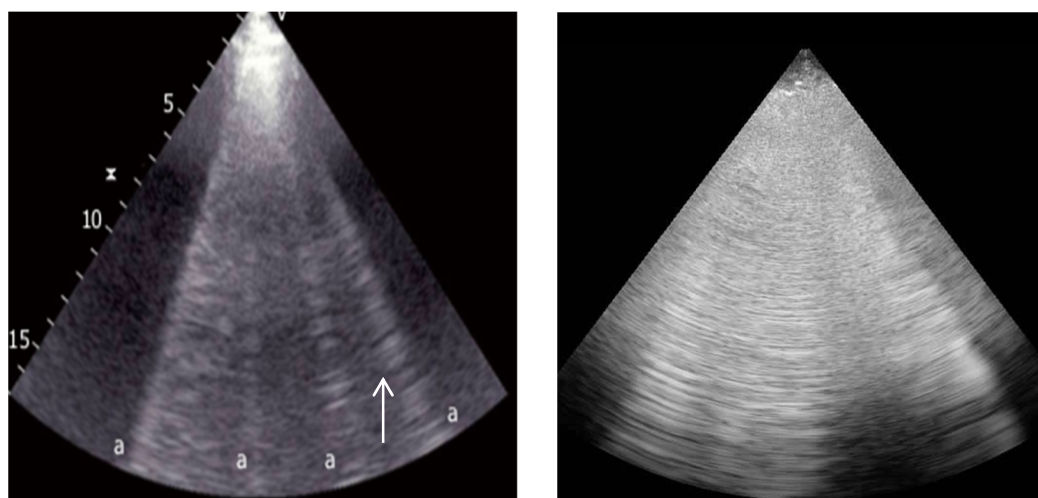


**Figure 4.** B-lines (left, indicated by arrow) and “B-pattern” (right).

### 2.3.2. Lung Consolidation

Lung consolidation corresponds to a complete loss of lung tissue aeration, which favors ultrasound transmission and is a common finding in various clinical conditions: pneumonia, atelectasis, and pulmonary embolisms [30]. In LUS examinations, a “tissue-like pattern” is defined as a homogeneous pattern in a lobe (Figure 5), similar to an abdominal organ parenchyma in the B-mode, and constitutes a real lung anatomical image [20,32]. The “tissue-like pattern” allows one to confirm community-acquired pneumonia diagnoses (sensitivity of 94–99% and specificity of 95–97%) [33,34]. Furthermore, the “shred sign” represents small subpleural consolidation, which is defined by a hypoechoic image delimited by irregular rims in the B-mode. The “shred sign” alone is not highly specific and, conversely, together with a “tissue-like pattern”, supports, with a higher diagnostic accuracy, lung consolidation diagnoses (sensitivity of 90% and specificity of 98%) [35]. Air bronchograms correspond to the air trapped within the lung consolidation region and are defined by linear hyperechoic images within a “tissue-like pattern” [36]. Air bronchograms allow one to distinguish between pneumonia and atelectasis, conditions that share lung consolidation, during LUS examinations [6]. A dynamic air bronchogram, defined by 1 mm of movement during inspiration, corresponds to patent airways and is suggestive of pneumonia with good specificity, ruling out atelectasis (sensitivity of 64% and specificity of 94%) [37]. Atelectasis is a complete loss of aeration within part of the lung or the whole lung. In LUS examinations, atelectasis shows lung consolidation with a “tissue-like pattern” and is associated with the absence of both lung sliding and dynamic air bronchograms [38].

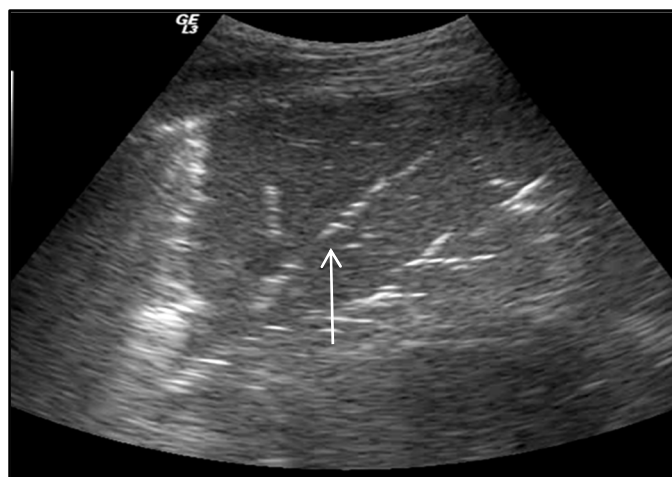


**Figure 5.** “Tissue-like pattern” with air bronchogram inside (arrow).

### 2.3.3. Pulmonary Embolism

For pulmonary embolisms, LUS exams can show the pulmonary infarction area, defined as triangular or rounded, hypoechoic, homogeneous subpleural consolidation [39]. A meta-analysis by Squizzato et al. [40] revealed an overall 87% sensitivity and 82% specificity for pulmonary embolism diagnoses using LUS examinations. According to the BLUE protocol, the combination of an LUS with venous ultrasonography can improve the specificity for pulmonary embolism diagnoses compared to an LUS alone (sensitivity of 81% and specificity of 99%) [1].

## 3. Cardiac Ultrasounds in the Emergency Department

### 3.1. Rationale and Methodology

The principal role of POCUS in the emergency department is the rapid assessment of patients with hemodynamic instabilities [41] through standardized protocols such as the RUSH (rapid ultrasound for shock and hypotension) and the E-FAST protocols (extended focused assessment with sonography in trauma).

Cardiac POCUS is done by using a low-frequency phased array probe (3.5–5 MHz) pointed at four main views: the parasternal long-axis, parasternal short-axis, apical four-chamber, and subcostal/subxiphoid views.

### 3.2. Shock

Shock is a high-mortality syndrome characterized by cellular hypoxia, which can be due to respiratory failure, increased oxygen consumption, or an inadequate supply of O<sub>2</sub> caused by cardiocirculatory failure and tissue hypoperfusion. This condition is defined by the coexistence of hypotension (systolic BP < 90 mmHg and mean BP < 65 mmHg), tachycardia (HR > 100), and signs of peripheral and central hypoperfusion [42]. There are four main physiopathological settings of shock (Table 1):

- Distributive.
- Hypovolemic.
- Obstructive.
- Cardiogenic.

POCUS is useful in the early identification of the etiology and of the pathophysiology of shock in the emergency room; in establishing the hemodynamic status through an estimation of the CVP, PWCP, SVR, and CO; in monitoring the patient; and in guiding the therapy [43,44]. In this setting, the RUSH protocol was developed to guide the user in the evaluation of critically ill patients in the stressful emergency setting [45]. This protocol aids the investigation of the most common causes of shock through the evaluation of LV and RV systolic dysfunction and cardiac tamponade (Table 2).

**Table 1.** Types of Shock [Mcgee W., Adler A., Sharma R., et al. Hemodynamic Assessment and Monitoring in the Intensive Care Unit: an Overview. Journal of Anesthesiology and Critical Care 01 Aug 2014. Doi:10.18650/2374-4448.14010].

Types of Shock		
Type	Etiology	Hemodynamics
Distributive	Septic, neurogenic, anaphylactic.	↓ SVR ↓ CVP ↓ PWCP ↑ CO (Hyperdynamic state) ↓ CO (Hypodynamic state)
Hypovolemic	Hemorrhagic, dehydration, third space sequestration.	↑ SVR ↓ CVP ↓ PWCP ↓ CO
Cardiogenic	Myocardial infarction, advanced heart failure, brady/tachyarrhythmias, valvular disease.	↑ SVR ↑ CVP ↑ PCWP (LV dysfunction) ↓ PCWP (RV dysfunction) ↓ CO
Obstructive	Heart tamponade, pulmonary embolism, tense pneumothorax, constrictive pericarditis, restrictive cardiomyopathy.	↑ SVR ↓ CVP ↓ PCWP (RV dysfunction) ↑ PCWP ↓ CO

Abbreviations: CO represents cardiac output, CVP represents central venous pressure, PVR represents peripheral vascular resistance, and PWCP represents pulmonary capillary wedge pressure.

**Table 2.** RUSH protocol. Echography finding in different types of shock [45].

RUSH Protocol				
	Hypovolemic	Distributive	Cardiogenic	Obstructive
<b>Pump</b>	- Hypercontractility. - Small dimensions of LV. - "Kissing" LV walls in systole.	- Hyper- or hypocontractility.	- Hypocontractility. - Normal dimensions or dilation of LV.	- Dyskinetic RV (McConnell's sign). - Intraventricular thrombus. - Cardiac tamponade.
<b>Tank</b>	- Small or virtual IVC. - Look for pleural and peritoneal fluid.	- Normal or small IVC. - Look for causes of sepsis.	- Dilated and hypocollapsing IVC. - Look for ascites, pleural effusion, and pulmonary congestion.	- Dilated and hypocollapsing IVC. - Look for PNx (Lung point).
<b>Pipes</b>	- Aortic aneurism. - Aortic dissection.	- Normal.	- Normal.	- DVT.

Abbreviations: DVT represents deep-vein thrombosis, IVC represents inferior vena cava, LV represents left ventricle, and PNx represents pneumothorax.

**(A) Estimation of CVP and of blood volume**

An estimation of the CVP/RAP (right atrial pressure) can be done through an evaluation of the anteroposterior diameter and grade of collapsibility of the IVC (inferior vena cava) in the subcostal view: a low preload (CVP 0–5 mmHg) is associated with a small diameter of the IVC (<10 mm) and the complete collapse of the IVC with inspiration. A high preload (CVP > 10 mmHg) is characterized by a dilated IVC (>20 mm) and a hypo- (<50%) or noncollapsing IVC [46]. This method is an easy and fast way to assess the patient's preload and to rule out hypovolemic shock.

**(B) Fluid responsiveness and stroke volume evaluation**

An examination of the IVC alone could fail to answer whether a hemodynamically unstable patient needs to be loaded with fluid [47]. Fluid responsiveness is defined as an increase of 15% in the cardiac output after a rapid infusion of crystalloids (4–7 mL/kg

in 15 min) or 1–2 min after a leg-raising test [48]. An echography evaluation of fluid responsiveness necessitates the application of the continuity equation to calculate the stroke volume (SV) variation before and after the volume challenge tests; thus, an evaluation of the LVOT systolic diameter in the parasternal long-axis view would be necessary to estimate the LVOT cross-sectional area ( $CSA_{LVOT}$ ) and the velocity–time integral of the power Doppler of the LVOT that was sampled from the center of the LVOT with a good alignment with the blood flow (normally obtained in the apical five-chamber view):

$$CSA_{LVOT} = (\pi (LVOT/2))^2; SV = CSA_{LVOT} \times VTI_{LVOT}; CO = SV \times HR$$

In consideration of the complexity of the evaluation of the LVOT diameter in critically ill patients and of the fact that small measurement errors would be elevated to the second power, we could simplify the equation by comparing the variations of the LVOT VTI or of the sole maximum velocities. This evaluation alone can give the emergency physician extremely important information on the hemodynamics of the patients and on the need for fluid implementation or diuretics administration.

### (C) Cardiac chambers size and systolic function

An evaluation of the cardiac chamber sizes and biventricular systolic function is of paramount importance in the etiologic diagnosis of hemodynamically unstable patients [49]. In the emergency setting, the LV global ejection fraction is estimated qualitatively as “normal”, “moderately reduced”, or “severely reduced” through an evaluation of the systolic–diastolic fractional shortening of the cavity diameter of the LV, which has shown an adequate correlation with cardiologists’ echocardiographic evaluations [49]. Thus, the identification of reduced LV systolic function can orient the physician towards the diagnosis of cardiogenic shock and indicates a need for further inotropes, for mechanical support, and for an emergent coronary angiographic evaluation [50]. In the evaluation of the RV, it is important to focus on the chamber dimensions (generally 2/3 of the left ventricle size in the apical four-chamber view) and the shape since a D-shaped appearance (Figure 6), associated with septal systolic bulging towards the left ventricle, is suggestive of a high-pressure regimen in the right heart, which could be associated with severe pulmonary hypertension or a pulmonary embolism [51]. RV systolic function can be estimated by evaluating the reduction of the cavity area (normal  $> 1/3$ ) and the tricuspid lateral annular plane excursion in the M-mode (TAPSE  $> 15$  mm). A dyskinetic RV could suggest the presence of a specific etiology: McConnell’s sign, described as right ventricular free-wall hypokinesia and normal apical contractility, is a specific sign of a pulmonary embolism if associated with RV dilatation and a coherent clinical setting of dyspnea and deep-vein thrombosis (DVT) [52].



**Figure 6.** Systolic bowing of interventricular septum towards the left ventricle (D-shape) is associated with pulmonary embolism and pulmonary hypertension.

**(D) Diastolic function and Wedge pressure**

The diastolic function of the LV can be grossly evaluated in the apical four-chamber view by focusing on the left atrium's dimensions and through the analysis of the pulsed-wave Doppler (PW) of the transmitral diastolic flow obtained by positioning the volume sample at the tip of the mitral leaflet [53]. The ratio between the protodiastolic E wave and the end-diastolic A wave gives preliminary information on the diastolic function of the heart (fig.). The evaluation of the mitral, annular, septal, and lateral protodiastolic mean velocity through the tissue Doppler technique permits the estimation of the LV diastolic filling pressures by using the E/e' ratio:

- An E/e' < 8 is generally associated with a normal PWCP.
- An E/e' > 15 is associated with a high PWCP.
- An E/e' between 8 and 15 necessitates a multiparametric evaluation of diastolic function.

This information is useful in guiding the treatment of the patient since, in the setting of diastolic dysfunction, with an augmented estimated PWCP, we could expect scarce or no response to fluid administration, while it could be beneficial to unload left heart filling pressures with diuretic therapy. Moreover, the position of the interatrial septum (IAS) can also be helpful: IAS bulging towards the right is a sign of elevated filling pressures in the left cardiac chambers.

**(E) Pericardium**

Emergency-room-focused ultrasounds, using the RUSH protocol or the FAST protocol (described below), permit the detection of pericardial effusion (PE) with an acceptable sensitivity and specificity (Figure 7). The subcostal view can be performed relatively easily in supine patients and is the most appropriate way to diagnose PE, which is visualized as an echo-free space between the heart and the parietal layer of the pericardium. Once a PE diagnosis has been made, the characterization of the fluid and the search for signs of possible cardiac tamponade must be performed by an expert echocardiographer. Pericardial tamponade is a clinical diagnosis that includes hemodynamic instability, pulsus paradoxus, jugular distension [54], and echographic evidence of PE associated with diastolic right chamber collapses and a dilated hypocoappling IVC.



**Figure 7.** Pericardial tamponade: end-diastolic right ventricular chamber collapse is associated with significant pericardial effusion.

If an emergency pericardiocentesis is indicated, POCUS can be useful for guiding the insertion of the needle into the pericardial space and for verifying whether the needle is

in the pericardial cavity after the infusion of agitated saline solution (Figure 8) [55]. Echo-guided pericardiocentesis have been shown to have an increased possibility of the success of the procedure and a reduced risk of complications when compared to the non-echo-guided procedure [56].



**Figure 8.** Bubble test during pericardiocentesis: appearance of bubbles in the pericardium (arrow) indicates that the needle is correctly positioned in the pericardial space.

### 3.3. Cardiac Arrest

The patient in cardiac arrest requires a prompt-initiation cardiopulmonary resuscitation (CRP) and Advanced Cardiac Life Support (ACLS) treatment algorithms. In this setting, POCUS could be a useful tool for guiding lifesaving bedside procedures (i.e., pericardiocentesis), for assessing the quality of chest compressions, for confirming the clinical suspect of a reversible cause of CA, and for differentiating true pulseless electrical activity (PEA) from pseudo-PEA [57]. The most recent European resuscitation council guidelines from 2021 [58], which are in line with an ILCOR systematic review [59], recommend the cautious use of POCUS in CA; in particular, no POCUS finding indicative of myocardial infarction, cardiac tamponade, hypovolemia, tension pneumothoraces, or pulmonary embolisms had a sufficiently high sensitivity or specificity to be used as the sole criterion for terminating CPR or for one to “rule out” or “rule in” the cause of cardiac arrest during resuscitation, especially in the absence of the clinical suspicion of a specific reversible cause [60]. For this reason, it is of paramount importance that the image acquisition and evaluation should be carried out by an expert echocardiographer, and it must not interfere with the quality of the resuscitation maneuvers. More specifically the subxiphoid view generally offers good visualization of the IVC, the pericardium, and the heart chambers and valves without impeding chest compressions; thus, it can give immediate information regarding the presence or absence of pericardial effusion, the volume status of the individual, and the quality of the chest compressions, while other views can be utilized in case of a specific clinical suspect and during the reevaluation of the cardiac rhythm. It is important to consider that the dilatation of the RV in the case of cardiac arrest has a low predictive value in diagnosing a pulmonary embolism since it is more probably caused by hypovolemia, hyperkalemia, and ventricular fibrillation, which may occur during cardiac arrest [61]. The possibility of differentiating the electromechanical dissociation of heart activity (PEA) from pseudo-PEA using echography is of particular interest. PEA is characterized by the presence of QRS in an EKG and the absence of cardiac contraction, while pseudo-PEA is defined by the absence of a pulse despite the presence of ventricular contractility being visualized on a cardiac

ultrasound. These patients have minimal cardiac output and have a higher survival rate, in part because there are often reversible causes for their arrest that can be identified with POCUS and treated adequately, improving the prognosis and the return to spontaneous circulation [60].

#### 4. Point-of-Care Abdominal Ultrasound

The most common POCUS applications of abdominal ultrasounds include the evaluation of patients with abdominal pain or trauma [62,63]. Moreover, POCUS has also been recently used to estimate patients' fluid status, especially in those with acutely decompensated heart failure and acute kidney injury. A low-frequency (3.5–5 MHz) curvilinear probe is most often used for abdominal USs thanks to its greater depth of penetration, although a linear probe transducer (high-frequency, 5–15 MHz) may be necessary in appendicitis and pediatric applications [64].

##### 4.1. Acute Abdominal Pain

Acute abdominal pain represents one of the most common causes of referrals to an emergency department, and POCUS provides help in differentiating patients who require additional diagnostic tests or hospitalization [65,66]. In this setting, US exams can identify intra-abdominal fluids, an aneurysm of the abdominal aorta, and hydronephrosis, and it can also provide important information about patients with trauma [3,67].

##### (A) Intraperitoneal free fluid

Abdominal ultrasounds allow for the detection of pathological intraperitoneal free fluid (IPF) accumulation, although it cannot differentiate the type of liquid. IPF may result from a ruptured ectopic pregnancy, a urine leak, bile, or ascites. IPF appears anechoic and is most often localized in the perihepatic (in Morrison's pouch) or perisplenic region, while, in the pelvis, it is usually seen in the pouch of Douglas. Therefore, it is important for evaluating the right upper quadrant (RUQ), left upper quadrant (LUQ), periphery of the abdomen (left and right) in the paracolic gutters, and pelvis. Once the fluid is localized, ultrasonographic guidance can increase success and decrease the complications of common procedures such as paracentesis [68]. Most often, IPF may result from thoracic or abdominal trauma. In this setting, focused assessments with sonography (FAST) quickly help to identify the intra-abdominal source of bleeding [3,4]. Indeed, FAST represents a rapid US exam performed by clinicians with the aim to rapidly evaluate patients suspected to have intra-abdominal or intrathoracic free fluid collection or cardiac tamponade. There is also the extended FAST (eFAST) protocol, which includes some additional ultrasound views to identify pneumothoraces [14,15].

##### (B) Appendicitis and Cholecystitis

USs of the right upper quadrant in people suspected to have biliary colic can reveal cholecystitis with a great accuracy [69,70]. Its diagnosis is suggested through the direct visualization of gallstones, which are seen as hyperechoic focuses with posterior shadowing (Figure 9), thickened and stratified gall bladder walls (Fig B), pericholecystic fluid, and a positive sonographic Murphy's sign [71]. POCUS performed by emergency physician has been shown to be as accurate as radiology ultrasounds in the diagnosis of cholecystitis [72,73], although, sometimes, US interpretation may be challenging owing to the absence of gallstones.

Several studies have demonstrated that the sensitivity and specificity of POCUS in detecting appendicitis are nearly 84% and 90%, respectively [74,75]. When evaluable, the appendix should be examined in the longitudinal and transverse planes [76]. Appendicitis is suspected when a US reveals a dilated noncompressible lumen with a maximum diameter higher than six millimeters, the presence of an appendicolith, and the "Target sign" in the transverse view (Figure 10). However, appendix examinations with USs are affected by the patient body weight, anatomical variants, and operator experience [77].

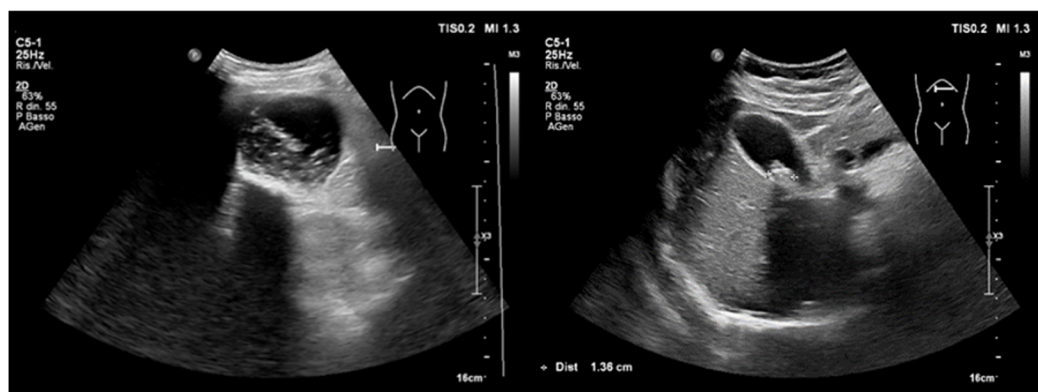


**Figure 9.** Ultrasonography of the right upper quadrant. A distended gallbladder with microlithiasis and large biliary sludge (left); multiple stones with posterior shadowing in the infundibulum (right).



**Figure 10.** Ultrasonography of normal and abnormal appendixes. On the left, there are longitudinal and transverse USs of acute appendicitis showing thickened walls and diameter > 6 mm. On the right, there is a thinner normal appendix.

### (C) Abdominal aortic aneurysm

POCUS represents an important tool for the diagnosis of abdominal aortic aneurysms in patients admitted into the emergency room for abdominal pain [78]. An AAA is defined as a permanent segmental dilatation of the abdominal aorta which most often involves the infrarenal segment with a maximum diameter over 30 mm. Moreover, large AAAs (over 55 mm) are at a high risk of rupture and should be considered for surgical repair [79]. US examinations must be performed from the epigastrium to the distal bifurcation, and they should describe the aorta's caliber and shape and differentiate between flap dissection and thrombosis within its lumen [80,81]. Furthermore, an AAA rupture and hemoperitoneum should always be ruled out [3].

#### 4.2. Acute Kidney Injury

An acute kidney injury is a common finding among patients admitted to the emergency department, but it portends a bad prognosis and a high mortality rate (about 50%) [82]. Bedside ultrasounds represent an important tool for investigating the etiology of AKIs and for guiding the most appropriate management technique [83].

##### 4.2.1. Hemodynamic AKI

A hemodynamic AKI is due to kidney hypoperfusion, and it may be due to volume depletion; cardiac dysfunction; severe abdominal congestion; or vasoplegia, such as in sepsis. A comprehensive assessment of the heart, lung water, and venous congestion [84] is essential to finding the etiology and to guiding therapy (i.e., decongestion, fluid resuscitation, or vasopressor agents) [85] as already discussed [48].

#### 4.2.2. Obstructive AKI

POCUS may quickly identify acute urinary retention and detect obstructive nephropathy requiring procedural drainage [86]. Nephrolithiasis is suggested through the direct visualization of stones [87] or through evidence of indirect signs of obstruction, such as hydronephrosis (Figure 11) or the absence of ureterovesical jets (UVJs). UVJs represent a surrogate for ureteral flow into the bladder, and their absence is most often suggestive of ureterolithiasis [88]. However, obstructive AKIs may be functional or due to intrinsic causes. In this case USs may demonstrate urinary tract dilatation at various levels without the finding of stones.

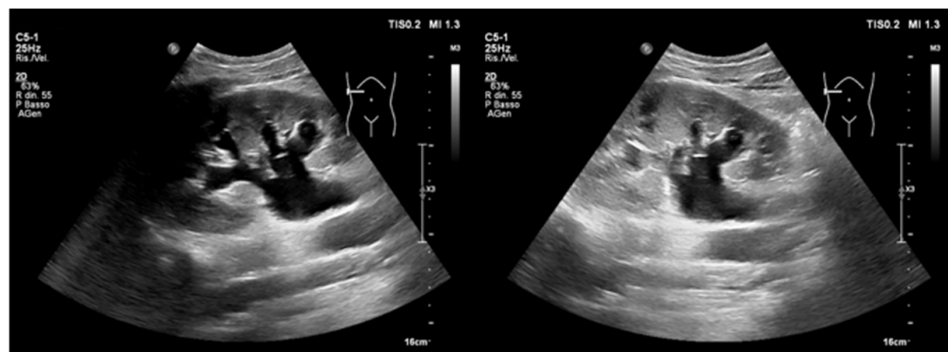


**Figure 11.** Pelvis and caliceal dilatation with proximal ureteral stone.

#### 4.2.3. Renal Resistive Index

Renal vascular studies also give useful information through the assessment of the renal resistive index (RRI). The RRI evaluates the macrovascular perfusion into the kidney [89] and is calculated from the following formula:

$$\text{RRI} = [\text{Peak systolic velocity (PSV)} - \text{End-diastolic velocity (EDV)}] / \text{Peak systolic velocity (PSV)},$$

where the PSV and EDV are obtained at the level of segmental arteries. A greater difference between the peak systolic velocity and end-diastolic velocity leads to a higher RRI and reflects a resistance to the blood flow [90]. The RRI is most often augmented either in intrinsic AKIs or in conditions with an elevated intrabdominal pressure, such as hepatorenal syndrome [91]. Moreover, it has been shown to be predictive of renal outcomes in selected patients [92,93].

#### 4.2.4. Chronic Kidney Disease

Renal ultrasonography provides information on the chronicity of medical renal disease through the evaluation of the renal length, the cortical thickness, and its echogenicity [94]. Hence, the presence of a thinned cortex together with a decreased kidney length suggest chronic kidney disease (CKD). Moreover, in CKD, the cortex appears more echogenic when compared to the liver or spleen even though increased echogenicity is subjective and can be skewed by liver disease [95].

#### 4.3. Point-of-Care Venous Doppler Ultrasound

An elevated right atrial pressure portends bad clinical outcomes in selected patients [96]. Venous point-of-care Doppler ultrasonography is emerging as a valuable bedside diagnostic tool for the assessment of fluid overloads, especially in acutely decompensated heart failure [97]. Abnormal flow patterns in hepatic, portal, and intrarenal veins waves have been linked to an elevated RAP, thus providing additive information about end-organ congestion [84]. In brief, congestion indicates poor outcomes in heart failure patients; therefore, a comprehensive assessment of the heart, lung water, and venous congestion permits the real-time evaluation of the efficacy of deresuscitation therapy and bears prognostic significance [84,98].

#### 4.3.1. Inferior Vena Cava

Although the IVC is a good indicator of the central venous pressure (CVP) [99], it is not always reliable for assessing the fluid status, such as assessing that in patients with lung hyperinflation (COPD and asthma), ventilator support, or cardiac conditions impeding the venous return (i.e., RV myocardial infarction and cardiac tamponade) [100]. However, a plethoric IVC (>2.1 cm) with a 50% inspiratory collapse usually indicates a high RAP of 15 mmHg (10–20 mm Hg) [101].

#### 4.3.2. Hepatic Vein Flow

The blood flow patterns in the hepatic veins (HVs) are pulsatile with two retrograde “A” and “V” waves and two anterograde “S” (systolic) and “D” (diastolic) waves. The S wave is larger than the D wave, and they represent the systolic movement of the anulus towards the apex and the diastolic ventricular filling, respectively. When the RAP increases, the amplitude of the S wave decreases when compared to that of the D wave (S < D pattern). As congestion worsens, the S wave becomes blunted until it is reversed [102]. Despite the fluid status, a systolic flow reversal is often observed in severe tricuspid regurgitation, whereas, in advanced pulmonary hypertension, A waves appear elevated together with decreased D wave amplitudes because of the elevated RV end-diastolic pressure [103].

#### 4.3.3. Portal Vein Flow

The portal vein (PV) is isolated from the central veins; therefore, its normal flow pattern appears continuous or mildly pulsatile. The main alteration in the PV waveform is the progressive pulsatility with an increasing RAP, which can be quantified using the pulsatility fraction [104].

PF:  $[(V_{\max} - V_{\min})/V_{\max}] \times 100$ ; a PF  $\geq 30\%$  is considered mild, whereas a PF  $\geq 50\%$  is considered severe.

Moreover, an increased pulsatility in the PV waveform is associated with a higher N-terminal pro-brain natriuretic peptide and worse clinical outcomes in heart failure patients if present at discharge [105].

#### 4.3.4. Intrarenal Vein Flow

A normal intrarenal vein Doppler (IRVD) is like that of the portal vein with a continuous flow and a brief interruption during atrial systole [106]. This pattern becomes biphasic with an increased RAP, and two distinct waves (S and D) can be observed, leaving only the diastolic component as congestion worsens (Figure 12). However, an IVRD is, most often, difficult to obtain, and it may be affected by other pathologies, such as severe TR or pulmonary hypertension, despite the volume status. IVRD is also strongly associated with clinical outcomes in HF patients [96].

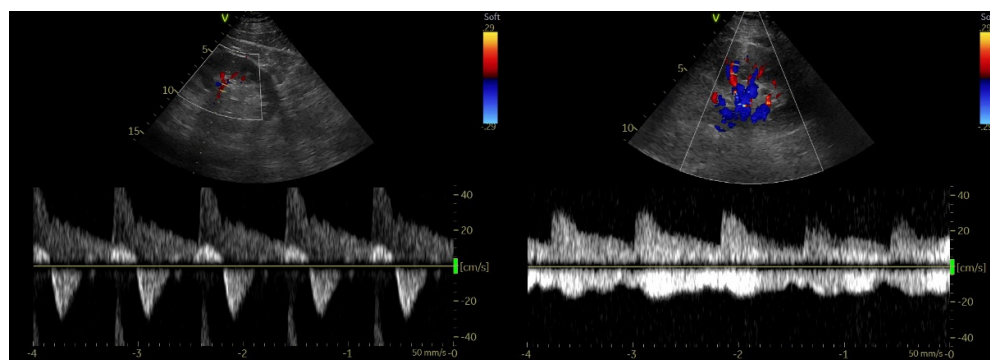


**Figure 12.** Intrarenal vein Doppler (above baseline) in a patient with acutely decompensated heart failure before (left) and after (right) decongestive therapy. The flow pattern appears monophasic/diastolic (L), becoming continuous as congestion reduces (R).

## 5. Deep-Vein Thrombosis

Acute lower-extremity proximal deep-vein thrombosis (DVT) represents the third leading vascular disease after acute myocardial infarction and stroke [107]. Although phlebography is the gold standard for the diagnosis of DVT [108], ultrasonography has become the standard in clinical practice due to cost effectiveness, quickness, and its simplicity of execution [109,110]. Several studies have shown that POCUS has the same diagnostic power as that of RUSs (radiology department ultrasounds) and venography even when performed in the emergency department [111–113].

### 5.1. Protocol

Regarding the instrumentation, the ultrasound machines used range from pocket-sized handset devices to advanced and more sophisticated devices [114]. It is appropriate to perform venous ultrasounds using a linear probe (5–10 MHz) and to set a scan depth from 1 to 4 cm. The position of the patient is certainly important for the correct performance of the examination. The bed must be at the proper height to promote operator comfort. The patient must lie supine with the head slightly elevated while in the “frog leg” position: this consists of extrarotating the thigh and flexing the leg slightly to allow better access to the inguinal region and to the popliteal fossa [114]. The two principal POCUS examination methods studied and applied for the diagnosis of deep-vein thrombosis are the “2-points” and “3-points” exams [115]. Despite the definition, both methods also consider multiple scan points. The diagnosis of deep-vein thrombosis can be performed through the direct visualization of the thrombus. The presence of an anechoic thrombus can be pointed out by performing a “compression ultrasound” (Figure 13): the absence of a reduction in the vessel caliber during compression is a clear sign of DVT [114]. Specifically, the “2-point” POCUS method explores the common femoral vein and popliteal vein [116]. In the “3-point” protocol, the technique is the same as that of the “2-point” examination of the femoral and popliteal veins with the addition of an adjunct projection to scan the proximal region of the femoral vein.

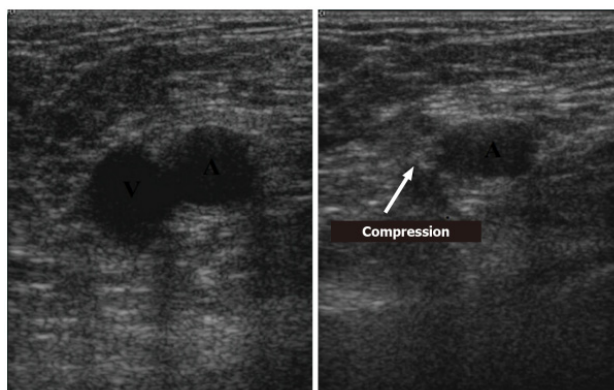


**Figure 13.** Compression ultrasound [Di Vilio A, Vergara A, Desiderio A, et al.: “A. Incremental value of compression ultrasound sonography in the emergency department. World J Crit Care Med. 2021 Sep 9;10(5):194–203].

### 5.2. Imaging

The natural history of deep-vein thrombosis goes through several stages: an initial phase (1–6 days) which is characterized by a mobile hypoechoic clot at high risk for embolism; a second stage (within two weeks) that involves a nonhomogeneous structure with mixed echogenicity (Figure 14); and a third and fourth stage (after two weeks) involving thrombus organization and vessel recanalization. Therefore, it is possible to see the flow entering inside of the clot by using the color Doppler technique. The ultrasound stages can be summarized as follows [110]:

1. Acute: the thrombus itself may not be visible. If detected, it is deformable with the force applied on the probe and with a regular surface; it is a distended vein.
2. Subacute thrombus: (before six months and after clot formation) intermediate morphological changes that cannot be included in the chronic phase.
3. Chronic post-thrombotic change: not compressible nor deformable with an irregular surface; the vein caliber may be normal or reduced.

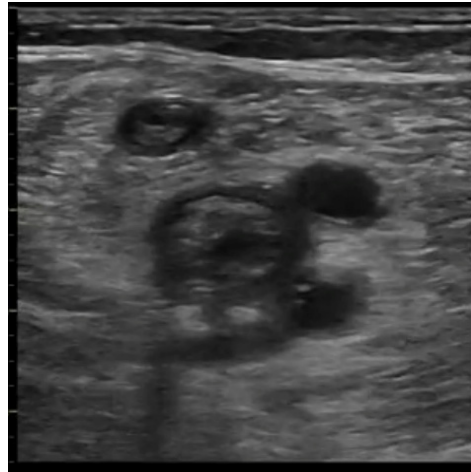


**Figure 14.** The image shows the presence of an extensive thrombus with mixed echogenicity occupying the lumen of the femoral vein and the great saphenous vein.

### 5.3. Accuracy of POCUS in Detecting a Pulse during Cardiac Arrest

Assessing the presence or absence of a pulse is a key moment in the management of cardiac arrest. Doppler ultrasounds provide an alternative to the manual pulse check. Sanchez et al. [117] conducted a cross-sectional multipatient, multireader repeated-measures diagnostic study in which they showed that the diagnostic ability to identify carotid pulse restoration during cardiac arrest is far superior in ultrasounds vs. palpation. Similarly, Choen et al. showed how Doppler ultrasounds on the femoral site are more accurate than manual palpation in identifying the presence of a pulse in patients admitted to the ED with cardiac arrest. It has been shown that a cut-off value of the peak systolic velocity of 20 cm/s correlates with a systolic blood pressure value of >60 mmHg [118]. POCUS on the carotid artery has also been evaluated to assess the carotid artery pulsatility during cardiac arrest [119], and it has been shown to rapidly identify the presence of a carotid pulse and, thus, predict ROSC.

### 5.4. TIA/Stroke Clinical Setting

In the clinical setting of suspected stroke or TIA in the emergency department, the POCUS method appears to have a poor correlation with CT for the diagnosis of significant stenosis [120]. Even though Saxhaug et al. showed how the technique is applicable to ruling out significant carotid artery pathology [121], further research and investigation are needed before the extensive use of carotid POCUS in patients with symptoms suggestive of acute cerebral ischemia is carried out.

## 6. Emerging Settings for POCUS Employment in Clinical Practice

### 6.1. Intracranial Pressure Monitoring

POCUS is currently used in various neurological settings, such as intracranial pressure (ICP) estimation, especially after a traumatic brain injury [122]. Even though invasive monitoring devices represent the gold standard, brain ultrasonography (BU) can be used as a valid alternative for intracranial pressure estimation [123]. An increase in the ICP results in the distension of the optic nerve sheath (ONS); therefore, changes in the ONS diameter correlate with ICP variation [124,125]. The ONS diameter (ONSD) can be assessed through

the transorbital window using a 2 MHz frequency ultrasound probe. The ONSD is measured behind the globe, using the optic disc as a reference point together with the central retinal artery color Doppler technique, which helps to identify the optic nerve [126]. Moreover, the blood flow velocities in the main cerebral arteries, measured through the transcranial Doppler (TCD) technique, help to identify intracranial hypertension by identifying an elevation in both the pulsatility index (PI) and the resistive index (RI) ([127,128]. In brief, the combination of data such as an optic nerve sheath diameter (ONSD) of >6 mm and a pulsatility index (PI) of >1.4 strongly correlates with an intracranial pressure of >22 mmHg, which identifies intracranial hypertension [129].

#### 6.2. Guidance for Invasive Procedures in Critically ill Patients

POCUS also allows one to verify the correct placement of the central venous catheter (CVC) through a saline flush test with evidence of a rapid atrial vortex within 2 s of starting the saline infusion from one of the CVC lumens [130]. Compared to chest radiography, POCUS allows one to verify the CVC position without radiation and with the possibility of identifying complications (e.g., pneumothoraces) in less time and with a noninferior sensitivity [131,132]. Furthermore, in ICUs, upper-airway POCUS provides valid support in the case of difficult intubations, such as those in patients with anatomies distorted by diseases or trauma, where POCUS helps to evaluate the depth of the endotracheal tube or to guide percutaneous tracheostomies [133].

#### 6.3. Chest Traumatology

POCUS is also acquiring an emerging role in chest traumatology. In particular, rib fractures are frequent complications of blunt chest trauma [134]. An early diagnosis associated with prompt measures to monitor possible chest trauma complications are essential in the critical care setting [135,136]. POCUS is performed at the site of the patient's maximal pain. A high-frequency linear probe is positioned perpendicularly to the long axis of the rib. This allows one to identify a hyperechoic structure and its acoustic shadowing, enabling differential diagnoses with adjacent pleural lines [137,138]. Through a US, a rib fracture can be identified as a break in the anterior hyperechoic margin of the rib. The entire rib is explored, and multiple views can be obtained in real time. In the presence of a rib fracture, POCUS can be useful for detecting other associated chest trauma complications, such as PNXs [139] and hemothoraces [140]. Radiography could miss rib fracture diagnoses, especially if these occur in the costal cartilages [141]. In fact, only 49% of rib fractures can be detected by physical evaluations and radiographs [142]. Conversely, POCUS had a sensitivity of 91.2% and a specificity of 72.7% in diagnosing rib fractures [143]. However, pain related to probe pressure [144] and inaccessible but uncommon fracture sites, such as the retroscapular ribs and the infraclavicular segment of the first rib, could represent major limitations to POCUS examinations [145].

#### 6.4. The emerging Role of Artificial Intelligence in POCUS

The implementation of artificial intelligence (AI) software in POCUS is undoubtedly fascinating and carries a great potential improvement to this methodology. The field of the application of machine learning and of deep learning software in echography could be directed at the training of resident physician [146]; nonetheless, it can support expert physicians in the emergency setting in reducing the duration of the exam via automated measurements with a reduction in the interoperator variability [147]. Several FDA approved machine learning softwares are already implemented in modern echography devices as reported by Knackstedt et al. [148], and the automeasurement of the left ventricular ejection fraction, of the left ventricle end-systolic and end-diastolic volumes, and of the global longitudinal strain showed a consistent agreement with manual measurements. Similarly, an auto-LVOT-VTI calculating software presented a good correlation with thermodilution cardiac output measurements [149]. Moreover, Zhang et al. [150] found that a deep learning software using convolutional neural networks (CNNs) had a 96% accuracy in discrim-

inating the echocardiographic view and a high accuracy in diagnosing several cardiac structural abnormalities. Artificial intelligence may hasten lung ultrasound evaluations through the automatic calculation of the Lung Ultrasound Score (LUS) and by helping in the discrimination of A-lines, B-lines, consolidation, and pleural effusion, with a potential utility in the emergency setting and in COVID-19 patients [151–153]. In the present day, AI can represent a promising tool for the improvement of POCUS evaluations, but it still needs further development and the implementation of large datasets to become an ally of the physician.

## 7. Conclusions

POCUS represents a goal-directed ultrasound examination which allows clinicians to rapidly evaluate patients in the emergency setting through a limited and focused number of standard echographic views. POCUS helps to make quick diagnoses and to identify early life-threatening conditions which require prompt interventions. The aim of our review was to summarize the various POCUS applications with a focus on the emergency setting as discussed below. Indeed, even if initially meant for cardiac and lung disease evaluations, US exams have been extended to many medical conditions with great clinical benefits both in the emergency setting and in critically ill patients. These considerations make ultrasonography an integral part of emergency medicine.

**Author Contributions:** Conceptualization, A.D. (Antonello D'Andrea) and C.D.G.; writing—original draft preparation, A.D. (Antonello D'Andrea), C.D.G., D.F., A.C., L.C. and F.S.; writing—review and editing, S.P., E.T. and A.D. (Alfonso Desiderio); visualization and supervision B.L., V.R. and A.D. (Antonello D'Andrea). All authors have read and agreed to the published version of the manuscript.

**Funding:** This research received no external funding.

**Institutional Review Board Statement:** Not applicable.

**Informed Consent Statement:** Not applicable.

**Data Availability Statement:** Not applicable.

**Conflicts of Interest:** The authors declare no conflict of interest.

## References

1. American College of Emergency Physicians. ACEP emergency ultrasound guidelines 2001. *Ann. Emerg. Med.* **2001**, *38*, 470–481. [[CrossRef](#)]
2. Whitson, M.R.; Mayo, P.H. Ultrasonography in the emergency department. *Crit. Care* **2016**, *20*, 1–8. [[CrossRef](#)] [[PubMed](#)]
3. Manson, W.C.; Kirksey, M.; Boublik, J.; Wu, C.L.; Haskins, S.C. Focused assessment with sonography in trauma (FAST) for the regional anesthesiologist and pain specialist. *Reg. Anesth. Pain Med.* **2019**, *44*, 540–548. [[CrossRef](#)] [[PubMed](#)]
4. Bahner, D.; Blaivas, M.; Cohen, H.L.; Fox, J.C.; Hoffenberg, S.; Kendall, J.; Langer, J.; McGahan, J.P.; Sierzenski, P.; Tayal, V.S.; et al. AIUM Practice Guideline for the Performance of the Focused Assessment with Sonography for Trauma (FAST) Examination. *J. Ultrasound Med.* **2008**, *27*, 313–318. [[CrossRef](#)]
5. Lichtenstein, D.A.; Mezière, G.A. Relevance of Lung Ultrasound in the Diagnosis of Acute Respiratory Failure: The BLUE Protocol. *Chest* **2008**, *134*, 117–125. [[CrossRef](#)] [[PubMed](#)]
6. Volpicelli, G.; Elbarbary, M.; Blaivas, M.; Lichtenstein, D.A.; Mathis, G.; Kirkpatrick, A.W.; Melniker, L.; Gargani, L.; Noble, V.E.; Via, G.; et al. International evidence-based recommendations for point-of-care lung ultrasound. *Intensive Care Med.* **2012**, *38*, 577–591. [[CrossRef](#)]
7. Volpicelli, G.; Cardinale, L.; Garofalo, G.; Veltri, A. Usefulness of lung ultrasound in the bedside distinction between pulmonary edema and exacerbation of COPD. *Emerg. Radiol.* **2008**, *15*, 145–151. [[CrossRef](#)]
8. Demi, L.; Wolfram, F.; Klersy, C.; De Silvestri, A.; Ferretti, V.V.; Muller, M.; Miller, D.; Feletti, F.; Welnicki, M.; Buda, N.; et al. New International Guidelines and Consensus on the Use of Lung Ultrasound. *J. Ultrasound Med.* **2022**, *42*, 309–344. [[CrossRef](#)]
9. Lichtenstein, D.; Meziere, G.; Biderman, P.; Gepner, A.; Barrè, O. The comet- tail artifact: An ultrasound sign of alveolar-interstitial syndrome. *Am. J. Respir. Crit. Care Med.* **1997**, *156*, 1640–1646. [[CrossRef](#)]
10. Lichtenstein, D.A.; Mezière, G.; Lascols, N.; Biderman, P.; Courret, J.-P.; Gepner, A.; Goldstein, I.; Tenoudji-Cohen, M. Ultrasound diagnosis of occult pneumothorax. *Crit. Care Med.* **2005**, *33*, 1231–1238. [[CrossRef](#)]
11. Lichtenstein, D.A.; Menu, Y. A bedside ultrasound sign ruling out pneumothorax in the critically ill: Lung sliding. *Chest* **1995**, *108*, 1345–1348. [[CrossRef](#)]

12. Lichtenstein, D.; Mezière, G.; Biderman, P.; Gepner, A. The “lung point”: An ultrasound sign specific to pneumothorax. *Intensive Care Med.* **2000**, *26*, 1434–1440. [[CrossRef](#)]
13. Chiumello, D.; Mongodi, S.; Algeri, I.; Vergani, G.L.; Orlando, A.; Via, G.; Crimella, F.; Cressoni, M.; Mojoli, F. Assessment of Lung Aeration and Recruitment by CT Scan and Ultrasound in Acute Respiratory Distress Syndrome Patients. *Crit. Care Med.* **2018**, *46*, 1761–1768. [[CrossRef](#)]
14. Lichtenstein, D.; Mezière, G.; Biderman, P.; Gepner, A. The comet-tail artifact: An ultrasound sign ruling out pneumothorax. *Intensive Care Med.* **1999**, *25*, 383–388. [[CrossRef](#)]
15. Blaivas, M.; Lyon, M.; Duggal, S. A prospective comparison of supine chest radiography and bedside ultrasound for the diagnosis of traumatic pneumothorax. *Acad. Emerg. Med.* **2005**, *12*, 844–849. [[CrossRef](#)]
16. Lichtenstein, D.A.; Lascols, N.; Prin, S.; Mezière, G. The “lung pulse”: An early ultrasound sign of complete atelectasis. *Intensive Care Med.* **2003**, *29*, 2187–2192. [[CrossRef](#)]
17. Volpicelli, G.; Boero, E.; Sverzellati, N.; Cardinale, L.; Busso, M.; Boccuzzi, F.; Tullio, M.; Lamorte, A.; Stefanone, V.; Ferrari, G.; et al. Semi-quantification of pneumothorax volume by lung ultrasound. *Intensive Care Med.* **2014**, *40*, 1460–1467. [[CrossRef](#)]
18. Doust, B.D.; Baum, J.K.; Maklad, N.F.; Doust, V.L. Ultrasonic evaluation of pleural opacities. *Radiology* **1975**, *114*, 135–140. [[CrossRef](#)]
19. Lichtenstein, D.A. Lung Ultrasound in the Critically Ill. *Ann. Intensive Care* **2014**, *4*, 1–12. [[CrossRef](#)]
20. Lichtenstein, D.; Goldstein, I.; Mourgeon, E.; Cluzel, P.; Grenier, P.; Rouby, J.-J. Comparative Diagnostic Performances of Auscultation, Chest Radiography, and Lung Ultrasonography in Acute Respiratory Distress Syndrome. *Anesthesiology* **2004**, *100*, 9–15. [[CrossRef](#)]
21. Lichtenstein, D. Should lung ultrasonography be more widely used in the assessment of acute respiratory disease? *Expert Rev. Respir. Med.* **2010**, *4*, 533–538. [[CrossRef](#)] [[PubMed](#)]
22. Yousefifard, M.; Baikpour, M.; Ghelichkhani, P.; Asady, H.; Nia, K.S.; Jafari, A.M.; Hosseini, M.; Safari, S. Screening Performance Characteristic of Ultrasonography and Radiography in Detection of Pleural Effusion; a Meta-Analysis. *Emergency* **2016**, *4*, 1–10. [[PubMed](#)]
23. Bouhemad, B.; Zhang, M.; Lu, Q.; Rouby, J.-J. Clinical review: Bedside lung ultrasound in critical care practice. *Crit. Care* **2007**, *11*, 205. [[CrossRef](#)] [[PubMed](#)]
24. Eibenberger, K.L.; Dock, W.I.; Ammann, M.E.; Dorffner, R.; Hormann, M.F.; Grabenwoger, F. Quantification of pleural effusions: Sonography versus radiography. *Radiology* **1994**, *191*, 681–684. [[CrossRef](#)] [[PubMed](#)]
25. Roch, A.; Bojan, M.; Michelet, P.; Romain, F.; Bregeon, F.; Papazian, L.; Auffray, J.P. Usefulness of ultrasonography in predicting pleural effusions > 500 mL in patients receiving mechanical ventilation. *Chest* **2005**, *127*, 224–232. [[CrossRef](#)]
26. Remerand, F.; Dellamonica, J.; Mao, Z.; Rouby, J.J. Direct bedside quantification of pleural effusion in ICU: A new sonographic method. *Intensive Care Med.* **2006**, *32*, S220.
27. Lichtenstein, D.; Hulot, J.-S.; Rabiller, A.; Tostivint, I.; Mezière, G. Feasibility and safety of ultrasound-aided thoracentesis in mechanically ventilated patients. *Intensive Care Med.* **1999**, *25*, 955–958. [[CrossRef](#)]
28. Lichtenstein, D. FALLS-protocol: Lung ultrasound in hemodynamic assessment of shock. *Heart Lung Vessel.* **2013**, *5*, 142–147.
29. Lichtenstein, D.; Mezière, G. A lung ultrasound sign allowing bedside distinction between pulmonary edema and COPD: The comet-tail artifact. *Intensive Care Med.* **1998**, *24*, 1331–1334. [[CrossRef](#)]
30. Volpicelli, G.; Caramello, V.; Cardinale, L.; Mussa, A.; Bar, F.; Frascisco, M.F. Detection of sonographic B-lines in patients with normal lung or radiographic alveolar consolidation. *J. Pharmacol. Exp. Ther.* **2008**, *14*, 122–128.
31. Copetti, R.; Soldati, G.; Copetti, P. Chest sonography: A useful tool to differentiate acute cardiogenic pulmonary edema from acute respiratory distress syndrome. *Cardiovasc. Ultrasound* **2008**, *6*, 16. [[CrossRef](#)]
32. Yang, P.C.; Chang, D.B.; Yu, C.J.; Lee, Y.C.; Kuo, S.H.; Luh, K.T. Ultrasound guided percutaneous cutting biopsy for the diagnosis of pulmonary consolidations of unknown aetiology. *Thorax* **1992**, *47*, 457–460. [[CrossRef](#)]
33. Reissig, A.; Copetti, R.; Mathis, G.; Mempel, C.; Schuler, A.; Zechner, P.; Aliberti, S.; Neumann, R.; Kroegel, C.; Hoyer, H. Lung ultrasound in the diagnosis and follow-up of community-acquired pneumonia: A prospective, multicenter, diagnostic accuracy study. *Chest* **2012**, *142*, 965–972. [[CrossRef](#)]
34. Cortellaro, F.; Colombo, S.; Coen, D.; Duca, P. Lung ultrasound is an accurate diagnostic tool for the diagnosis of pneumonia in the emergency department. *Emerg. Med. J.* **2010**, *29*, 19–23. [[CrossRef](#)]
35. Lichtenstein, D.A.; Lascols, N.; Mezière, G.; Gepner, A. Ultrasound diagnosis of alveolar consolidation in the critically ill. *Intensive Care Med.* **2004**, *30*, 276–281. [[CrossRef](#)]
36. Weinberg, E.D.B.; Diakoumakis, E.; Kassner, E.; Seife, B.; Zvi, Z.; Kurian, J.; Levin, T.L.; Han, B.K.; Taragin, B.H.; Weinstein, S.; et al. The air bronchogram: Sonographic demonstration. *Am. J. Roentgenol.* **1986**, *147*, 593–595. [[CrossRef](#)]
37. Lichtenstein, D.; Mezière, G.; Seitz, J. The dynamic air bronchogram: A lung ultrasound sign of alveolar consolidation ruling out atelectasis. *Chest* **2009**, *135*, 1421–1425. [[CrossRef](#)]
38. Lee, F.C.Y. Lung ultrasound—A primary survey of the acutely dyspneic patient. *J. Intensive Care* **2016**, *4*, 57. [[CrossRef](#)]
39. Shrestha, G.S. Point-of-care Ultrasonography in Critically Ill Patients. *Kathmandu Univ. Med. J.* **2015**, *13*, 83–87. [[CrossRef](#)]
40. Squizzato, A.; Rancan, E.; Dentali, F.; Bonzini, M.; Guasti, L.; Steidl, L.; Mathis, G.; Ageno, W. Diagnostic accuracy of lung ultrasound for pulmonary embolism: A systematic review and meta-analysis. *J. Thromb. Haemost.* **2013**, *11*, 1269–1278. [[CrossRef](#)]

41. Labovitz, A.J.; Noble, V.E.; Bierig, M.; Goldstein, S.A.; Jones, R.; Kort, S.; Porter, T.R.; Spencer, K.T.; Tayal, V.S.; Wei, K. Focused Cardiac Ultrasound in the Emergent Setting: A Consensus Statement of the American Society of Echocardiography and American College of Emergency Physicians. *J. Am. Soc. Echocardiogr.* **2010**, *23*, 1225–1230. [[CrossRef](#)] [[PubMed](#)]
42. Cibinel, G.A. POCUS shock management: Point-of-care ultrasound in the integrated management of shock. *Ital. J. Emerg. Med.* **2022**, *11*, 57–71. [[CrossRef](#)]
43. Berg, I.; Walpot, K.; Lamprecht, H.; Valois, M.; Lanctôt, J.-F.; Srouf, N.; Brand, C.V.D. A Systemic Review on the Diagnostic Accuracy of Point-of-Care Ultrasound in Patients with Undifferentiated Shock in the Emergency Department. *Cureus* **2022**, *14*, e23188. [[CrossRef](#)] [[PubMed](#)]
44. Stickles, S.P.; Carpenter, C.R.; Gekle, R.; Kraus, C.K.; Scoville, C.; Theodoro, D.; Tran, V.H.; Ubiñas, G.; Raio, C. The diagnostic accuracy of a point-of-care ultrasound protocol for shock etiology: Asystematic review and meta-analysis. *Can. J. Emerg. Med.* **2019**, *21*, 406–417. [[CrossRef](#)] [[PubMed](#)]
45. Perera, P.; Mailhot, T.; Riley, D.; Mandavia, D. The RUSH Exam: Rapid Ultrasound in Shock in the Evaluation of the Critically Ill. *Emerg. Med. Clin.* **2010**, *28*, 29–56. [[CrossRef](#)]
46. Porter, T.R.; Shillcutt, S.K.; Adams, M.S.; Desjardins, G.; Glas, K.E.; Olson, J.J.; Troughton, R.W. Guidelines for the Use of Echocardiography as a Monitor for Therapeutic Intervention in Adults: A Report from the American Society of Echocardiography. *J. Am. Soc. Echocardiogr.* **2015**, *28*, 40–56. [[CrossRef](#)]
47. Kim, D.-W.; Chung, S.; Kang, W.-S.; Kim, J. Diagnostic Accuracy of Ultrasonographic Respiratory Variation in the Inferior Vena Cava, Subclavian Vein, Internal Jugular Vein, and Femoral Vein Diameter to Predict Fluid Responsiveness: A Systematic Review and Meta-Analysis. *Diagnostics* **2021**, *12*, 49. [[CrossRef](#)]
48. Monnet, X.; Shi, R.; Teboul, J.L. Prediction of fluid responsiveness. What's new? *Ann. Intensive Care* **2022**, *12*, 46. [[CrossRef](#)]
49. Lang, R.M.; Badano, L.P.; Mor-Avi, V.; Afilalo, J.; Armstrong, A.; Ernande, L.; Flachskampf, F.A.; Foster, E.; Goldstein, S.A.; Kuznetsova, T.; et al. Recommendations for Cardiac Chamber Quantification by Echocardiography in Adults: An Update from the American Society of Echocardiography and the European Association of Cardiovascular Imaging. *J. Am. Soc. Echocardiogr.* **2015**, *28*, 1–39. [[CrossRef](#)]
50. Moore, C.L.; Rose, G.A.; Tayal, V.S.; Sullivan, D.M.; Arrowood, J.A.; Kline, J.A. Determination of Left Ventricular Function by Emergency Physician Echocardiography of Hypotensive Patients. *Acad. Emerg. Med.* **2002**, *9*, 186–193. [[CrossRef](#)]
51. Lodato, J.A.; Ward, R.P.; Lang, R.M. Echocardiographic predictors of pulmonary embolism in patients referred for helical CT. *Echocardiography* **2008**, *25*, 584–590. [[CrossRef](#)]
52. Konstantinides, S.; Meyer, G.; Becattini, C.; Bueno, H.; Geersing, G.-J.; Harjola, V.-P.; Huisman, M.; Humbert, M.; Jennings, C.S.; Jiménez, D.; et al. 2019 ESC Guidelines for the diagnosis and management of acute pulmonary embolism developed in collaboration with the European Respiratory Society (ERS). *Eur. Heart J.* **2020**, *41*, 543–603. [[CrossRef](#)]
53. Nagueh, S.F.; Appleton, C.P.; Gillebert, T.C.; Marino, P.N.; Oh, J.K.; Smiseth, O.A.; Waggoner, A.D.; Flachskampf, F.A.; Pellikka, P.A.; Evangelisa, A. Recommendations for the Evaluation of Left Ventricular Diastolic Function by Echocardiography: An Update from the American Society of Echocardiography and the European Association of Cardiovascular Imaging. *J. Am. Soc. Echocardiogr.* **2016**, *29*, 277–314. [[CrossRef](#)]
54. Saito, Y.; Donohue, A.; Attai, S.; Vahdat, A.; Brar, R.; Handapangoda, I.; Chandraratna, P.A. The syndrome of cardiac tamponade with “small” pericardial effusion. *Echocardiography* **2008**, *25*, 321–327. [[CrossRef](#)]
55. Ainsworth, C.D.; Salehian, O. Echo-guided pericardiocentesis: Let the bubbles show the way. *Circulation* **2011**, *123*, e210–e211. [[CrossRef](#)]
56. Flint, N.; Siegel, R.J. Echo-Guided Pericardiocentesis: When and How Should It Be Performed? *Curr. Cardiol. Rep.* **2020**, *22*, 1–9. [[CrossRef](#)]
57. Lalande, E.; Burwash-Brennan, T.; Burns, K.; Atkinson, P.; Lambert, M.; Jarman, B.; Lamprecht, H.; Banerjee, A.; Woo, M.Y. Is point-of-care ultrasound a reliable predictor of outcome during atraumatic, non-shockable cardiac arrest? A systematic review and meta-analysis from the SHoC investigators. *Resuscitation* **2019**, *139*, 159–166. [[CrossRef](#)]
58. Soar, J.; Böttiger, B.W.; Carli, P.; Couper, K.; Deakin, C.D.; Djäv, T.; Lott, C.; Olasveengen, T.; Paal, P.; Pellis, T.; et al. European Resuscitation Council Guidelines 2021: Adult advanced life support. *Resuscitation* **2021**, *161*, 115–151. [[CrossRef](#)]
59. Reynolds, J.C.; Issa, M.S.; Nicholson, T.C.; Drennan, I.R.; Berg, K.M.; O’Neil, B.J.; Welsford, M.; Andersen, L.W.; Böttiger, B.W.; Callaway, C.W.; et al. Prognostication with point-of-care echocardiography during cardiac arrest: A systematic review. *Resuscitation* **2020**, *152*, 56–68. [[CrossRef](#)]
60. Ávila-Reyes, D.; Acevedo-Cardona, A.O.; Gómez-González, J.F.; Echeverry-Piedrahita, D.R.; Aguirre-Flórez, M.; Giraldo-Diaconeasa, A. Point-of-care ultrasound in cardiorespiratory arrest (POCUS-CA): Narrative review article. *Ultrasound J.* **2021**, *13*, 46. [[CrossRef](#)]
61. Aagaard, R.; Granfeldt, A.; Bøtker, M.T.; Mygind-Klausen, T.; Kirkegaard, H.; Løfgren, B. The Right Ventricle Is Dilated during Resuscitation from Cardiac Arrest Caused by Hypovolemia: A Porcine Ultrasound Study. *Crit. Care Med.* **2017**, *45*, e963–e970. [[CrossRef](#)] [[PubMed](#)]
62. Radonjić, T.; Popović, M.; Zdravković, M.; Jovanović, I.; Popadić, V.; Crnokrak, B.; Klačnja, S.; Mandić, O.; Dukić, M.; Branković, M. Point-of-Care Abdominal Ultrasonography (POCUS) on the Way to the Right and Rapid Diagnosis. *Diagnostics* **2022**, *12*, 2052. [[CrossRef](#)] [[PubMed](#)]
63. Sternbach, G. Abdominal ultrasound in emergency medicine. *J. Emerg. Med.* **1984**, *1*, 547–548. [[CrossRef](#)] [[PubMed](#)]

64. Kameda, T.; Taniguchi, N. Overview of point-of-care abdominal ultrasound in emergency and critical care. *J. Intensive Care* **2016**, *4*, 1–9. [[CrossRef](#)]
65. Mazzei, M.A.; Guerrini, S.; Squitieri, N.C.; Cagini, L.; Macarini, L.; Coppolino, F.; Giganti, M.; Volterrani, L. The role of US examination in the management of acute abdomen. *Crit. Ultrasound J.* **2013**, *5*, S6. [[CrossRef](#)]
66. Abu-Zidan, F.M.; Khan, M.A.B. Point-of-care ultrasound for the acute abdomen in the primary health care. *Turk. J. Emerg. Med.* **2020**, *20*, 1–11. [[CrossRef](#)]
67. Holmes, J.F.; Harris, D.; Battistella, F.D. Performance of abdominal ultrasonography in blunt trauma patients with out-of-hospital or emergency department hypotension. *Ann. Emerg. Med.* **2004**, *43*, 354–361. [[CrossRef](#)]
68. Liu, R.B.; Donroe, J.H.; McNamara, R.L.; Forman, H.P.; Moore, C.L. The Practice and Implications of Finding Fluid during Point-of-Care Ultrasonography: A Review. *JAMA Intern. Med.* **2017**, *177*, 1818–1825. [[CrossRef](#)]
69. Kendall, J.L.; Shimp, R.J. Performance and interpretation of focused right upper quadrant ultrasound by emergency physicians. *J. Emerg. Med.* **2001**, *21*, 7–13. [[CrossRef](#)]
70. Zenobii, M.F.; Accogli, E.; Domanico, A.; Arienti, V. Update on bedside ultrasound (US) diagnosis of acute cholecystitis (AC). *Intern. Emerg. Med.* **2015**, *11*, 261–264. [[CrossRef](#)]
71. Summers, S.M.; Scruggs, W.; Menchine, M.D.; Lahham, S.; Anderson, C.; Amr, O.; Lotfipour, S.; Cusick, S.S.; Fox, J.C. A Prospective Evaluation of Emergency Department Bedside Ultrasonography for the Detection of Acute Cholecystitis. *Ann. Emerg. Med.* **2010**, *56*, 114–122. [[CrossRef](#)]
72. Scruggs, W.; Fox, J.C.; Potts, B.; Zlidenny, A.; McDonough, J.; Anderson, C.L.; Larson, J.; Barajas, G.; Langdorf, M.I. Accuracy of ED Bedside Ultrasound for Identification of gallstones: Retrospective analysis of 575 studies. *West. J. Emerg. Med.* **2008**, *9*, 1–5.
73. Benabbas, R.; Hanna, M.; Shah, J.; Sinert, R. Diagnostic Accuracy of History, Physical Examination, Laboratory Tests, and Point-of-Care Ultrasound for Pediatric Acute Appendicitis in the Emergency Department: A Systematic Review and Meta-Analysis. *Acad. Emerg. Med.* **2017**, *24*, 523–551. [[CrossRef](#)]
74. Lee, S.H.; Seong, J.Y. Diagnostic performance of emergency physician-performed point-of-care ultrasonography for acute appendicitis: A meta-analysis. *Am. J. Emerg. Med.* **2019**, *37*, 696–705. [[CrossRef](#)]
75. Fields, J.M.; Davis, J.; Alsup, C.; Bates, A.; Au, A.; Adhikari, S.; Farrell, I. Accuracy of Point-of-Care Ultrasonography for Diagnosing Acute Appendicitis: A Systematic Review and Meta-Analysis. *Acad. Emerg. Med.* **2017**, *24*, 1124–1136. [[CrossRef](#)]
76. Mostbeck, G.; Adam, E.J.; Nielsen, M.B.; Claudon, M.; Clevert, D.A.; Nicolau, C.; Nyhsen, C.; Owens, C.M. How to diagnose acute appendicitis: Ultrasound first. *Insights Imaging* **2016**, *7*, 255–263. [[CrossRef](#)]
77. Lam, S.H.; Grippo, A.; Kerwin, C.; Konicki, P.J.; Goodwine, D.; Lambert, M.J. Bedside Ultrasonography as an Adjunct to Routine Evaluation of Acute Appendicitis in the Emergency Department. *West. J. Emerg. Med.* **2014**, *15*, 808–815. [[CrossRef](#)]
78. Costantino, T.G.; Bruno, E.C.; Handly, N.; Dean, A.J. Accuracy of Emergency Medicine Ultrasound in the Evaluation of Abdominal Aortic Aneurysm. *J. Emerg. Med.* **2005**, *29*, 455–460. [[CrossRef](#)]
79. Moll, F.L.; Powell, J.T.; Fraedrich, G.; Verzini, F.; Haulon, S.; Waltham, M.; van Herwaarden, J.A.; Holt, P.J.E.; van Keulen, J.W.; Rantner, B.; et al. Management of Abdominal Aortic Aneurysms Clinical Practice Guidelines of the European Society for Vascular Surgery. *Eur. J. Vasc. Endovasc. Surg.* **2011**, *41*, S1–S58. [[CrossRef](#)]
80. Rubano, E.; Mehta, N.; Caputo, W.; Paladino, L.; Sinert, R. Systematic Review: Emergency Department Bedside Ultrasonography for Diagnosing Suspected Abdominal Aortic Aneurysm. *Acad. Emerg. Med.* **2013**, *20*, 128–138. [[CrossRef](#)]
81. Bravo-Merino, L.; González-Lozano, N.; Maroto-Salmón, R.; Mejjide-Santos, G.; Suárez-Gil, P.; Fañanás-Mastral, A. Validity of the Abdominal Ecography in Primary Care for Detection of Aorta Abdominal Aneurism in Male between 65 and 75 Years. *Aten. Primaria* **2019**, *51*, 11–17. [[CrossRef](#)] [[PubMed](#)]
82. Hoste, E.A.J.; Bagshaw, S.M.; Bellomo, R.; Cely, C.M.; Colman, R.; Cruz, D.N.; Edipidis, K.; Forni, L.G.; Gomersall, C.D.; Govil, D.; et al. Epidemiology of acute kidney injury in critically ill patients: The multinational AKI-EPI study. *Intensive Care Med.* **2015**, *41*, 1411–1423. [[CrossRef](#)] [[PubMed](#)]
83. Faubel, S.; Patel, N.U.; Lockhart, M.E.; Cadnapaphornchai, M.A. Renal Relevant Radiology: Use of Ultrasonography in Patients with AKI. *Clin. J. Am. Soc. Nephrol.* **2013**, *9*, 382–394. [[CrossRef](#)] [[PubMed](#)]
84. Argaiz, E.R.; Koratala, A.; Reisinger, N. Comprehensive Assessment of Fluid Status by Point-of-Care Ultrasonography. *Kidney360* **2021**, *2*, 1326–1338. [[CrossRef](#)] [[PubMed](#)]
85. Bissell, B.D.; Laine, M.E.; Thompson Bastin, M.L.; Flannery, A.H.; Kelly, A.; Riser, J.; Neyra, J.A.; Potter, J.; Morris, P.E. Impact of proto-colized diuresis for de-resuscitation in the intensive care unit. *Crit. Care* **2020**, *24*, 70. [[CrossRef](#)]
86. Smith-Bindman, R.; Aubin, C.; Bailitz, J.; Bengiamin, R.N.; Camargo, C.A.; Corbo, J.; Dean, A.J.; Goldstein, R.B.; Griffey, R.T.; Jay, G.D.; et al. Ultrasonography versus Computed Tomography for Suspected Nephrolithiasis. *N. Engl. J. Med.* **2014**, *371*, 1100. [[CrossRef](#)]
87. Wong, C.; Teitge, B.; Ross, M.; Young, P.; Robertson, H.L.; Lang, E. The Accuracy and Prognostic Value of Point-of-Care Ultrasound for Nephrolithiasis in the Emergency Department: A Systematic Review and Meta-Analysis. *Acad. Emerg. Med.* **2018**, *25*, 684–698. [[CrossRef](#)]
88. Fields, J.M.; Fischer, J.I.; Anderson, K.L.; Mangili, A.; Panebianco, N.L.; Dean, A.J. The ability of renal ultrasound and ureteral jet evaluation to predict 30-day outcomes in patients with suspected nephrolithiasis. *Am. J. Emerg. Med.* **2015**, *33*, 1402–1406. [[CrossRef](#)]
89. Capotondo, L.; Nicolai, G.A.; Garosi, G. The role of color Doppler in acute kidney injury. *Arch. Ital. Urol. Androl.* **2010**, *82*, 275–279.

90. Schnell, D.; Deruddre, S.; Harrois, A.; Pottecher, J.; Cosson, C.; Adoui, N.; Benhamou, D.; Vicaut, E.; Azoulay, E.; Duranteau, J. Renal resistive index better predicts the occurrence of acute kidney injury than cystatin C. *Shock* **2012**, *38*, 592–597. [[CrossRef](#)]
91. Umgelter, A.; Reindl, W.; Franzen, M.; Lenhardt, C.; Huber, W.; Schmid, R.M. Renal resistive index and renal function before and after paracentesis in patients with hepatorenal syndrome and tense ascites. *Intensive Care Med.* **2008**, *35*, 152–156. [[CrossRef](#)]
92. Iacoviello, M.; Monitillo, F.; Leone, M.; Citarelli, G.; Doronzo, A.; Antoncetti, V.; Puzzovivo, A.; Rizzo, C.; Lattarulo, M.S.; Massari, F.; et al. The Renal Arterial Resistance Index Predicts Worsening Renal Function in Chronic Heart Failure Patients. *Cardiorenal Med.* **2016**, *7*, 42–49. [[CrossRef](#)]
93. Goyal, S. Intrarenal resistance index (RI) as a predictor of early renal impairment in patients with liver cirrhosis. *Trop. Gastroenterol.* **2014**, *34*, 235–239. [[CrossRef](#)]
94. Beland, M.D.; Walle, N.L.; Machan, J.T.; Cronan, J.J. Renal Cortical Thickness Measured at Ultrasound: Is It Better Than Renal Length as an Indicator of Renal Function in Chronic Kidney Disease? *Am. J. Roentgenol.* **2010**, *195*, W146–W149. [[CrossRef](#)]
95. Yamashita, S.R.; Von Atzingen, A.C.; Iared, W.; Bezerra, A.S.D.A.; Ammirati, A.L.; Canziani, M.E.F.; D'Ippolito, G. Value of renal cortical thickness as a predictor of renal function impairment in chronic renal disease patients. *Radiol. Bras.* **2015**, *48*, 12–16. [[CrossRef](#)]
96. Beaubien-Souligny, W.; Benkreira, A.; Robillard, P.; Bouabdallaoui, N.; Chasse, M.; Desjardins, G.; Lamarche, Y.; White, M.; Bouchard, J.; Denault, A. Alterations in portal vein flow and intrarenal venous flow are associated with acute kidney injury after cardiac surgery: A prospective observational cohort study. *J. Am. Heart Assoc.* **2018**, *7*, e009961. [[CrossRef](#)]
97. Beaubien-Souligny, W.; Rola, P.; Haycock, K.; Bouchard, J.; Lamarche, Y.; Spiegel, R.; Denault, A.Y. Quantifying systemic congestion with Point-of-Care ultrasound: Development of the venous excess ultrasound grading system. *Ultrasound J.* **2020**, *12*, 1–12. [[CrossRef](#)]
98. Abhilash, K.; Kazory, A. Point of Care Ultrasonography for Objective Assessment of Heart Failure: Integration of Cardiac, Vascular, and Extravascular Determinants of Volume Status. *Cardiorenal Med.* **2021**, *11*, 5–17.
99. Saha, N.M.; Barbat, J.J.; Fedson, S.; Anderson, A.; Rich, J.D.; Spencer, K.T. Outpatient Use of Focused Cardiac Ultrasound to Assess the Inferior Vena Cava in Patients with Heart Failure. *Am. J. Cardiol.* **2015**, *116*, 1224–1228. [[CrossRef](#)]
100. Feissel, M.; Michard, F.; Faller, J.-P.; Teboul, J.-L. The respiratory variation in inferior vena cava diameter as a guide to fluid therapy. *Intensive Care Med.* **2004**, *30*, 1834–1837. [[CrossRef](#)]
101. Lombardi, A.; Gambardella, M.; Palermi, S.; Frecentese, F.; Serio, A.; Sperlongano, S.; Tavarozzi, R.; D'andrea, A.; De Luca, M.; Politi, C. Liver and heart failure: An ultrasound relationship. *J. Basic Clin. Physiol. Pharmacol.* **2022**. [[CrossRef](#)] [[PubMed](#)]
102. Singh, S.; Koratala, A. Utility of Doppler ultrasound derived hepatic and portal venous waveforms in the management of heart failure exacerbation. *Clin. Case Rep.* **2020**, *8*, 1489–1493. [[CrossRef](#)] [[PubMed](#)]
103. Zhang, A.; Himura, Y.; Kumada, T. The characteristics of hepatic venous flow velocity pattern in patients with pulmonary hypertension by pulsed Doppler echocardiography. *Jpn. Circ. J.* **1992**, *56*, 317–324.
104. Catalano, D.; Caruso, G.; Di Fazzio, S.; Carpinteri, G.; Scalisi, N.; Trovato, G.M. Portal vein pulsatility ratio and heart failure. *J. Clin. Ultrasound* **1998**, *26*, 27–31. [[CrossRef](#)]
105. Shih, C.Y.; Yang, S.S.; Hu, J.T.; Lin, C.L.; Lai, Y.C.; Chang, C.W. Portal vein pulsatility index is a more important indicator than congestion index in the clinical evaluation of right heart function. *World J. Gastroenterol.* **2006**, *12*, 768–771. [[CrossRef](#)]
106. Tang, W.H.W.; Kitai, T. Intrarenal venous flow: A window into the congestive kidney failure phenotype of heart failure? *JACC Heart Fail.* **2016**, *4*, 683–686. [[CrossRef](#)]
107. Di Nisio, M.; Van Es, N.; Büller, H.R. Deep vein thrombosis and pulmonary embolism. *Lancet* **2016**, *388*, 3060–3073. [[CrossRef](#)]
108. De Valois, J.C.; Schaik, C.C.; Verzijlbergen, F.; Ramshorst, B.; Eikelboom, B.C.; Meuwissen, O.J.A.T. Contrast venography: From gold standard to 'golden backup' in clinically suspected deep vein thrombosis. *Eur. J. Radiol.* **1990**, *11*, 131–137. [[CrossRef](#)]
109. Pomero, F.; Dentali, F.; Borretta, V.; Bonzini, M.; Melchio, R.; Douketis, J.D.; Fenoglio, L.M. Accuracy of emergency physician-performed ultrasonography in the diagnosis of deep-vein thrombosis: A systematic review and meta-analysis. *Thromb. Haemost.* **2013**, *109*, 137–145. [[CrossRef](#)]
110. Di Vilio, A.; Vergara, A.; Desiderio, A.; Iodice, F.; Serio, A.; Palermi, S.; Gambardella, F.; Sperlongano, S.; Gioia, R.; Acitorio, M.; et al. Incremental value of compression ultrasound sonography in the emergency department. *World J. Crit. Care. Med.* **2021**, *10*, 194–203. [[CrossRef](#)]
111. Magazzini, S.; Vanni, S.; Toccafondi, S.; Paladini, B.; Zanobetti, M.; Giannazzo, G.; Federico, R.; Grifoni, S. Duplex ultrasound in the emergency department for the diagnostic management of clinically suspected deep vein thrombosis. *Acad. Emerg. Med.* **2007**, *14*, 216–220. [[CrossRef](#)]
112. Burnside, P.R.; Brown, M.D.; Kline, J.A. Systematic review of emergency physician-performed ultrasonography for lower-extremity deep vein thrombosis. *Acad. Emerg. Med.* **2008**, *15*, 493–498. [[CrossRef](#)]
113. Canakci, M.E.; Acar, N.; Bilgin, M.; Kuas, C. Diagnostic value of point-of-care ultrasound in deep vein thrombosis in the emergency department. *J. Clin. Ultrasound* **2020**, *48*, 527–531. [[CrossRef](#)]
114. Varrias, D.; Palaiodimos, L.; Balasubramanian, P.; Barrera, C.A.; Nauka, P.; Arfaras-Melainis, A.; Zamora, C.; Zavras, P.; Napolitano, M.; Gulani, P.; et al. The Use of Point-of-Care Ultrasound (POCUS) in the Diagnosis of Deep Vein Thrombosis. *J. Clin. Med.* **2021**, *10*, 3903. [[CrossRef](#)]
115. Kline, J.A.; O'Malley, P.M.; Tayal, V.S.; Snead, G.R.; Mitchell, A.M. Emergency Clinician-Performed Compression Ultrasonography for Deep Venous Thrombosis of the Lower Extremity. *Ann. Emerg. Med.* **2008**, *52*, 437–445. [[CrossRef](#)]

116. Adhikari, S.; Zeger, W.; Thom, C.; Fields, J.M. Isolated Deep Venous Thrombosis: Implications for 2-Point Compression Ultrasonography of the Lower Extremity. *Ann. Emerg. Med.* **2015**, *66*, 262–266. [[CrossRef](#)]
117. Sanchez, S.; Miller, M.; Asha, S. Assessing the validity of two-dimensional carotid ultrasound to detect the presence and absence of a pulse. *Resuscitation* **2020**, *157*, 67–73. [[CrossRef](#)]
118. Cohen, A.L.; Li, T.; Becker, L.B.; Owens, C.; Singh, N.; Gold, A.; Nelson, M.J.; Jafari, D.; Haddad, G.; Nello, A.V.; et al. Femoral artery Doppler ultrasound is more accurate than manual palpation for pulse detection in cardiac arrest. *Resuscitation* **2022**, *173*, 156–165. [[CrossRef](#)]
119. Kang, S.Y.; Jo, I.J.; Lee, G.; Park, J.E.; Kim, T.; Lee, S.U.; Hwang, S.Y.; Shin, T.G.; Kim, K.; Shim, J.S.; et al. Point-of-care ultrasound compression of the carotid artery for pulse determination in cardiopulmonary resuscitation. *Resuscitation* **2022**, *179*, 206–213. [[CrossRef](#)]
120. Suttie, R.; Woo, M.Y.; Park, L.; Nemnom, M.-J.; Stotts, G.; Perry, J.J. Can Emergency Physicians Perform Carotid Artery Point-of-Care Ultrasound to Detect Stenosis in Patients with TIA and Stroke? A Pilot Study. *West. J. Emerg. Med.* **2020**, *21*, 626–632. [[CrossRef](#)]
121. Saxhaug, L.M.; Graven, T.; Olsen, O.; Kleinau, J.O.; Skjetne, K.; Ellekjær, H.; Dalen, H. Reliability and agreement of point-of-care carotid artery examinations by experts using hand-held ultrasound devices in patients with ischaemic stroke or transitory ischaemic attack. *Open Heart* **2022**, *9*, e001917. [[CrossRef](#)]
122. Caldas, J.; Rynkowski, C.B.; Robba, C. POCUS, how can we include the brain? An overview. *J. Anesth. Analg. Crit. Care* **2022**, *2*, 1–16. [[CrossRef](#)]
123. Meyfroidt, G.; Bouzat, P.; Casaer, M.P.; Chesnut, R.; Hamada, S.R.; Helbok, R.; Hutchinson, P.; Maas, A.I.R.; Manley, G.; Menon, D.K. Management of moderate to severe traumatic brain injury: An update for the intensivist. *Intensive Care Med.* **2022**, *48*, 649–666. [[CrossRef](#)]
124. Cannata, G.; Pezzato, S.; Esposito, S.; Moscatelli, A. Optic Nerve Sheath Diameter Ultrasound: A Non-Invasive Approach to Evaluate Increased Intracranial Pressure in Critically Ill Pediatric Patients. *Diagnostics* **2022**, *12*, 767. [[CrossRef](#)] [[PubMed](#)]
125. Richards, E.; Munakomi, S.; Mathew, D. Optic Nerve Sheath Ultrasound. In *StatPearls*; StatPearls Publishing: Tampa, FL, USA, 2022.
126. Aslan, N.; Yıldızdaş, D.; Horoz, Ö.Ö.; Özsoy, M.; Yöntem, A.; Çetinalp, E.; Mert, G.G. Evaluation of ultrasonographic optic nerve sheath diameter and central retinal artery Doppler indices by point-of-care ultrasound in pediatric patients with increased intracranial pressure. *Turk. J. Pediatr.* **2021**, *63*, 300–306. [[CrossRef](#)] [[PubMed](#)]
127. D’Andrea, A.; Fabiani, D.; Cante, L.; Caputo, A.; Sabatella, F.; Riegler, L.; Alfano, G.; Russo, V. Transcranial Doppler ultrasound: Clinical applications from neurological to cardiological setting. *J. Clin. Ultrasound* **2022**, *50*, 1212–1223. [[CrossRef](#)] [[PubMed](#)]
128. Bouzat, P.; Oddo, M.; Payen, J.F. Transcranial Doppler after traumatic brain injury: Is there a role? *Curr. Opin. Crit. Care* **2014**, *20*, 153–160. [[CrossRef](#)] [[PubMed](#)]
129. Robba, C.; Pozzebon, S.; Moro, B.; Vincent, J.-L.; Creteur, J.; Taccone, F.S. Multimodal non-invasive assessment of intracranial hypertension: An observational study. *Crit. Care* **2020**, *24*, 1–10. [[CrossRef](#)]
130. Duran-Gehring, P.E.; Guirgis, F.W.; McKee, K.C.; Goggans, S.; Tran, H.; Kalynych, C.J.; Wears, R.L. The bubble study: Ultrasound confirmation of central venous catheter placement. *Am. J. Emerg. Med.* **2015**, *33*, 315–319. [[CrossRef](#)]
131. Montrief, T.; Alerhand, S.; Denault, A.; Scott, J. Point-of-care echocardiography for the evaluation of right-to-left cardiopulmonary shunts: A narrative review. *Can. J. Anesth.* **2020**, *67*, 1824–1838. [[CrossRef](#)]
132. Amir, R.; Knio, Z.O.; Mahmood, F.; Oren-Grinberg, A.; Leibowitz, A.; Bose, R.; Shaefi, S.; Mitchell, J.D.; Ahmed, M.; Bardia, A.; et al. Ultrasound as a Screening Tool for Central Venous Catheter Positioning and Exclusion of Pneumothorax. *Crit. Care Med.* **2017**, *45*, 1192–1198. [[CrossRef](#)]
133. Osman, A.; Sum, K.M. Role of upper airway ultrasound in airway management. *J. Intensive Care* **2016**, *4*, 1–7. [[CrossRef](#)]
134. Hurley, M.E.; Keye, G.D.; Hamilton, S. Is ultrasound really helpful in the detection of rib fractures? *Injury* **2004**, *35*, 562–566. [[CrossRef](#)]
135. Cameron, P.; Dziukas, L.; Hadj, A.; Clark, P.; Hooper, S. Rib Fractures in Major Trauma. *Aust. N. Z. J. Surg.* **1996**, *66*, 530–534. [[CrossRef](#)]
136. Barnea, Y.; Kashtan, H.; Skornick, Y.; Werbin, N. Isolated rib fractures in elderly patients: Mortality and morbidity. *Can. J. Surg.* **2002**, *45*, 43–46.
137. Kara, M.; Dikmen, E.; Erdal, H.H.; Simsir, I.; Kara, S.A. Disclosure of unnoticed rib fractures with the use of ultrasonography in minor blunt chest trauma. *Eur. J. Cardio-Thorac. Surg.* **2003**, *24*, 608–613. [[CrossRef](#)]
138. Mathis, G. Thoraxsonography—Part I: Chest wall and pleura. *Ultrasound Med. Biol.* **1997**, *23*, 1131–1139. [[CrossRef](#)]
139. Chan, S.S. Emergency bedside ultrasound to detect pneumothorax. *Acad. Emerg. Med.* **2003**, *10*, 91–94. [[CrossRef](#)]
140. Ma, O.; Mateer, J.R. Trauma Ultrasound Examination Versus Chest Radiography in the Detection of Hemothorax. *Ann. Emerg. Med.* **1997**, *29*, 312–316. [[CrossRef](#)]
141. Turk, F.; Kurt, A.B.; Saglam, S. Evaluation by ultrasound of traumatic rib fractures missed by radiography. *Emerg. Radiol.* **2010**, *17*, 473–477. [[CrossRef](#)]
142. Crandall, J.; Kent, R.; Patrie, J.; Fertile, J.; Martin, P. Rib fracture patterns and radiologic detection—A restraint-based comparison. *Annu. Proc. Assoc. Adv. Automot. Med.* **2000**, *44*, 235–259. [[PubMed](#)]

143. Çelik, A.; Akoglu, H.; Omercikoglu, S.; Bugdayci, O.; Karacabey, S.; Kabaroglu, K.A.; Onur, O.; Denizbasi, A. The Diagnostic Accuracy of Ultrasonography for the Diagnosis of Rib Fractures in Patients Presenting to Emergency Department with Blunt Chest Trauma. *J. Emerg. Med.* **2021**, *60*, 90–97. [[CrossRef](#)] [[PubMed](#)]
144. Lalande, É.; Guimont, C.; Émond, M.; Parent, M.C.; Topping, C.; Kuimi, B.L.B.; Boucher, V.; Le Sage, N. Feasibility of emergency department point-of-care ultrasound for rib fracture diagnosis in minor thoracic injury. *Can. J. Emerg. Med.* **2017**, *19*, 213–219. [[CrossRef](#)] [[PubMed](#)]
145. Griffith, J.; Rainer, T.; Ching, A.S.; Law, K.L.; Cocks, R.A.; Metreweli, C. Sonography compared with radiography in revealing acute rib fracture. *Am. J. Roentgenol.* **1999**, *173*, 1603–1609. [[CrossRef](#)]
146. Narang, A.; Bae, R.; Hong, H.; Thomas, Y.; Surette, S.; Cadieu, C.; Chaudhry, A.; Martin, R.P.; McCarthy, P.M.; Rubenson, D.S.; et al. Utility of a Deep-Learning Algorithm to Guide Novices to Acquire Echocardiograms for Limited Diagnostic Use. *JAMA Cardiol.* **2021**, *6*, 624–632. [[CrossRef](#)]
147. Chen, X.; Owen, C.A.; Huang, E.C.; Maggard, B.D.; Latif, R.K.; Clifford, S.P.; Li, J.; Huang, J. Artificial Intelligence in Echocardiography for Anesthesiologists. *J. Cardiothorac. Vasc. Anesth.* **2021**, *35*, 251–261. [[CrossRef](#)]
148. Asch, F.M.; Abraham, T.; Jankowski, M.; Cleve, J.; Adams, M.; Romano, N.; Polivert, N.; Hong, H.; Lang, R. Accuracy and Reproducibility of a Novel Artificial Intelligence Deep Learning-Based Algorithm for Automated Calculation of Ejection Fraction in Echocardiography. *J. Am. Coll. Cardiol.* **2019**, *73*, 1447. [[CrossRef](#)]
149. Bobbia, X.; Muller, L.; Claret, P.-G.; Vigouroux, L.; Perez-Martin, A.; de La Coussaye, J.E.; Lefrant, J.Y.; Louart, G.; Roger, C.; Markarian, T. A New Echocardiographic Tool for Cardiac Output Evaluation: An Experimental Study. *Shock* **2019**, *52*, 449–455. [[CrossRef](#)]
150. Zhang, J.; Gajjala, S.; Agrawal, P.; Tison, G.H.; Hallock, L.A.; Beussink-Nelson, L.; Lassen, M.H.; Fan, E.; Aras, M.A.; Jordan, C.; et al. Fully Automated Echocardiogram Interpretation in Clinical Practice. *Circulation* **2018**, *138*, 1623–1635. [[CrossRef](#)]
151. Camacho, J.; Muñoz, M.; Genovés, V.; Herraiz, J.L.; Ortega, I.; Belarra, A.; González, R.; Sánchez, D.; Giacchetta, R.C.; Trueba-Vicente, A.; et al. Artificial Intelligence and Democratization of the Use of Lung Ultrasound in COVID-19: On the Feasibility of Automatic Calculation of Lung Ultrasound Score. *Int. J. Transl. Med.* **2022**, *2*, 17–25. [[CrossRef](#)]
152. Cho, Y.-J.; Song, K.-H.; Lee, Y.; Yoon, J.H.; Park, J.Y.; Jung, J.; Lim, S.Y.; Lee, H.; Yoon, H.I.; Park, K.U.; et al. Lung ultrasound for early diagnosis and severity assessment of pneumonia in patients with corona virus disease 2019. *Korean J. Intern. Med.* **2020**, *35*, 771–781. [[CrossRef](#)]
153. Russell, F.M.; Ehrman, R.R.; Barton, A.; Sarmiento, E.; Ottenhoff, J.E.; Nti, B.K. B-line quantification: Comparing learners novice to lung ultrasound assisted by machine artificial intelligence technology to expert review. *Ultrasound J.* **2021**, *13*, 1–7. [[CrossRef](#)]

**Disclaimer/Publisher’s Note:** The statements, opinions and data contained in all publications are solely those of the individual author(s) and contributor(s) and not of MDPI and/or the editor(s). MDPI and/or the editor(s) disclaim responsibility for any injury to people or property resulting from any ideas, methods, instructions or products referred to in the content.